

*Draft — August 19, 2020*  
Nature Reviews Earth & Environment

# **The Role of Mantle Plumes in Deep Earth and Surface Processes**

**Anthony A.P. Koppers**<sup>1\*</sup>, **Thorsten W. Becker**<sup>2</sup>, **Matthew G. Jackson**<sup>3</sup>  
**Kevin Konrad**<sup>1</sup>, **R. Dietmar Müller**<sup>4</sup>, **Barbara Romanowicz**<sup>5ABC</sup>  
**Bernhard Steinberger**<sup>6AB</sup>, **Joanne M. Whittaker**<sup>7</sup>

- <sup>1</sup> College of Earth, Ocean & Atmospheric Sciences  
Oregon State University  
104 CEOAS Administration Building, Corvallis, OR 97331-5503, USA  
ORCID ID# 0000-0002-8136-5372
- <sup>2</sup> Institute for Geophysics and Department of Geological Sciences  
Jackson School of Geosciences  
The University of Texas at Austin  
Austin TX 78758, USA
- <sup>3</sup> Department of Earth Science  
University of California, Santa Barbara  
Santa Barbara, CA 93109-9630, USA
- <sup>4</sup> EarthByte Group, School of Geosciences  
The University of Sydney  
Sydney, NSW 2006, Australia
- <sup>5A</sup> Department of Earth and Planetary Sciences  
University of California, Berkeley  
291 McCone Hall, Berkeley, CA 94720-4767, USA
- <sup>5B</sup> Collège de France, Paris (11 Place Marcelin Berthelot, 75005 Paris, France)
- <sup>5C</sup> Institut de Physique du Globe de Paris, 1 rue Jussieu, 75230 Paris CEDEX 05, France
- <sup>6A</sup> Hemholtz Centre Potsdam  
GFZ German Research Center for Geosciences  
Albert-Einstein-Straße 42-46, 14473 Potsdam, Germany
- <sup>6B</sup> Centre for Earth Evolution and Dynamics (CEED),  
Postbox 1028 Blindern, 0315 Oslo, Norway
- <sup>7</sup> Institute for Marine and Antarctic Studies  
University of Tasmania  
Hobart, Tasmania 7001, Australia
- \* Corresponding Author: [anthony.koppers@oregonstate.edu](mailto:anthony.koppers@oregonstate.edu)

## Key Messages

- 1 • Thermochemical mantle plumes are an integral part of a dynamic Earth's interior.
- 2 • Many mantle plumes originate from the deepest regions in Earth's mantle.
- 3 • Mantle plumes influence surface processes, including Earth's environment and climate.

## 1. Abstract

4 The existence of mantle plumes to explain intra-plate, hotspot volcanism was proposed half a century ago,  
5 but their role in Earth's mantle dynamics has been debated. Since then, our understanding of mantle  
6 processes has been informed by progress in seismic imaging, modelling of mantle flow in numerical and  
7 laboratory experiments, plate tectonic reconstructions, as well as the collection and interpretation of  
8 isotopic and geochronological data in ocean island basalts (OIB) and continental hotspot tracks. While the  
9 fine-scale structure of mantle plumes has yet to come into focus, seismological evidence for their  
10 presence, rooted at the core-mantle boundary, as proposed by Morgan (1971), is mounting. The classical  
11 model of purely thermal mantle plumes with narrow (~200 km) stems and large heads, rising vertically  
12 through the mantle right underneath all hotspot volcanoes, has been refined. Improved models  
13 substantiate that some plumes are thermochemical and can attain complex and broader shapes, that  
14 plumes are often not stationary but deflected in the mantle wind, and that many—but not all—plumes are  
15 rooted in a dense basal layer, likely of different composition than bulk mantle, and often as part of large  
16 regions characterized by anomalously low seismic velocities. Here, we review the recent evolution in our  
17 understanding of the morphology and composition of plumes, their role in global mantle convection, as  
18 well as how mantle plumes contribute to the long-term evolution of the mantle, and how they may impact  
19 climate, ocean chemistry, global biosystem evolution, and continental break-up. Our understanding of the  
20 nature and impact of mantle plumes has increased markedly, but more work is required to arrive at a  
21 deeper understanding of Earth's dynamic interior as connected to a large range of surface processes.

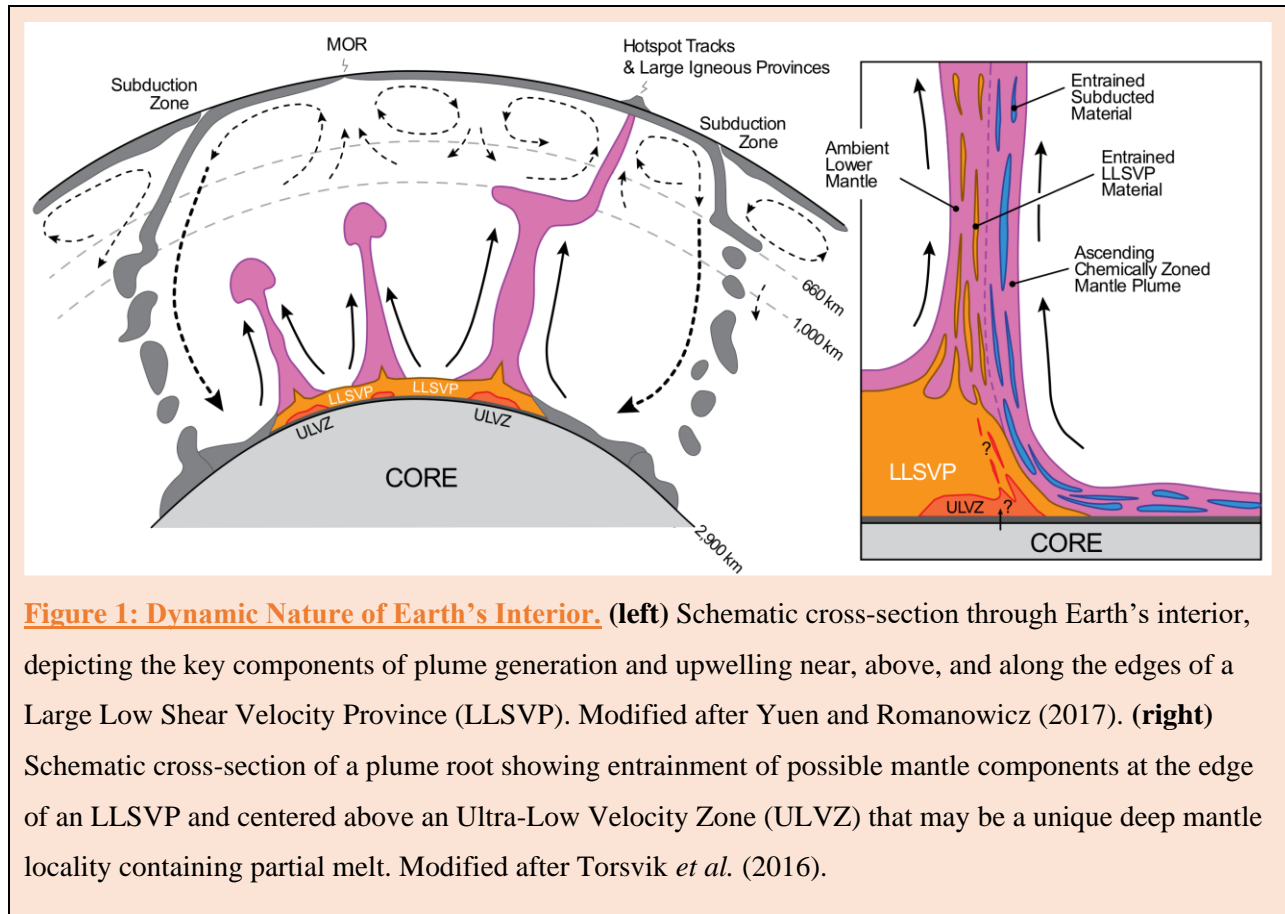
## 2. Introduction

22 Originally proposed to explain the existence of linear chains of intra-plate volcanoes with ages increasing  
23 in the direction of plate motion (Wilson 1963), mantle plumes have been classically defined as narrow,  
24 thermal upwellings, with large plume heads, as expected in a temperature dependent viscosity fluid of  
25 uniform composition that is heated from below. These plumes could start as deep as the core-mantle  
26 boundary (Morgan 1971) at roughly 2,900 km depth, rising to the base of Earth's lithosphere over tens of  
27 millions of years (**Figure 1a**). Here, partial melting of the plume material may result in magmatism that  
28 creates large igneous provinces (LIPs) and age-progressive volcanic chains for the plume head and tail,

29 respectively. This intra-plate volcanism, which typically forms away from and seemingly independent of  
30 major plate tectonic boundaries, may be the only means of directly sampling materials from the deepest  
31 mantle, and as such provides a unique ‘window’ into the workings and makeup of Earth’s interior.

32 Mantle upwellings, as an integral part of a convecting Earth, were first invoked in the first half of  
33 the 20th century. Alfred Wegener’s (1915) theory that continents drift over geological time required a  
34 driving mechanism that by some was imagined to involve whole mantle convection (Holmes 1928; 1931).  
35 The plate tectonics revolution in the 1960s provided an explanation for volcanism on plate boundaries,  
36 but not in the middle of plates. J. Tuzo Wilson (1963) and W. Jason Morgan (1971) hypothesized that the  
37 volcanic islands of Hawaii formed on a rigid tectonic plate moving over a ‘hotspot’ in the Earth’s  
38 asthenosphere, centered above a vertical, narrow, hot mantle plume from the deep mantle. Coming full  
39 circle, the deep mantle sources of these plumes were later connected to the existence of recycled ‘old’  
40 oceanic lithosphere (and sediments) that were conveyed to Earth’s deep interior via subduction and, over  
41 the course of hundreds of millions to billions of years, returned to the surface (Hofmann and White 1982;  
42 White and Hofmann 1982; Zindler and Hart 1986). If mantle plumes exist, the studies of their volcanic  
43 surface products, therefore, provide key insights into mantle dynamics, as well as insights into the  
44 convective scales of Earth’s very deep interior near the core-mantle boundary, and into the global  
45 geochemical cycle governed by downwelling at subduction zones and upwelling from a variety of large-  
46 scale chemical mantle reservoirs.

47 The dynamics of mantle upwellings and their relation with hotspots are still debated. It is unclear  
48 whether hotspot volcanism is sourced by broad upwellings, or narrower upwellings in the form of mantle  
49 plumes, or both. It is also debated whether some kinds of upwellings are confined to the upper mantle  
50 alone, above the seismic 660 km mantle discontinuity, or whether they are all sourced much deeper from  
51 near the core-mantle boundary (e.g. Richards *et al.* 1989; Davaille 1999; Steinberger 2000; Courtillot *et*  
52 *al.* 2003; Schubert *et al.* 2004; Koppers 2011; Anderson 2013; Anderson and Natland 2014; Konrad *et al.*  
53 2018a). How many mantle plumes exist, their longevity, dynamic behavior, and chemical make-up, are  
54 still poorly understood. While advocates for an important role of plumes in the physical and chemical  
55 evolution of the planet argue for connections between large-scale Earth processes, plate tectonics and  
56 volcanism, seismic tomography has only recently (Nelson and Grand 2018) imaged the first conduit that  
57 is sufficiently narrow that it could be a purely thermal mantle plume as proposed by Wilson and Morgan.  
58 Opponents of the plume concept have argued that, alternatively, near-surface processes, limited to Earth’s  
59 lithosphere, may explain the same observations (Foulger and Natland 2003; Anderson 2013).



67 Over the last decades, advanced computer modeling and laboratory experiments have shown how  
 68 entrainment of chemical heterogeneity may change the physical and chemical characteristics of plume  
 69 conduits, causing large variations in the behavior of the resulting ‘thermochemical’ plumes that are  
 70 dependent on various plate tectonic and geophysical boundary conditions (e.g. Olson and Yuen 1982;  
 71 Davaille 1999; Davaille *et al.* 2002; Jellinek and Manga 2004; Ballmer *et al.* 2011; Davies 2005;  
 72 Deschamps *et al.* 2011; Tan *et al.* 2011; Bossmann and van Keken 2013; Hassan *et al.* 2015). At the same  
 73 time, seismic tomography studies have pointed out the existence of two large anomalous domains in the  
 74 deepest parts of the mantle that show lower seismic velocities than surrounding regions (e.g. Dziewonski  
 75 and Woodhouse 1987; Li and Romanowicz 1996; Grand *et al.* 1997; van der Hilst *et al.* 1997; Su and  
 76 Dziewonski 1997; Masters *et al.* 2000; Ritsema *et al.* 2011). These domains are now referred to as "large  
 77 low shear velocity provinces" (LLSVPs) and some studies have proposed that they function as primary  
 78 plume nurseries. Notably, recent mantle tomography studies have shown the existence of broader ‘plume  
 79 like’ structures extending from the deep mantle in the vicinity of some hotspot volcanoes (Montelli *et al.*  
 80 2006; Boschi *et al.* 2008; French and Romanowicz 2015; Lei *et al.* 2020).

81 In this review, we discuss progress in imaging deep mantle structures, understanding their  
82 potential role in mantle plume formation, and modeling the shapes and behaviors of plumes depending on  
83 composition, rheology, and other boundary conditions. We discuss how the composition of oceanic island  
84 basalts increases our knowledge of deep mantle reservoirs and may provide geochemical evidence for  
85 plumes generated at the core-mantle boundary. We also discuss how paleomagnetic and age information  
86 in seamount chains inform past plate and plume motions, how and if true polar wander of our planet may  
87 happen given the observed overall mantle structure and behavior, and how continental break up and the  
88 formation of new ocean basins may occur when mantle plumes impinge on the base of Earth's  
89 lithosphere. Finally, we discuss how mantle plumes can influence the state of Earth's climate and ocean  
90 health on geological timescales.

### 3. Deep Mantle Superstructures

91 Based on today's global seismic tomography models we can recognize two large-scale features with  
92 anomalously low seismic velocities in the deepest parts of the mantle. Although the general outlines and  
93 locations underneath the Pacific and below Africa are generally agreed upon, the makeup and origin of  
94 these features (continuous piles versus plume bundles) are still debated as well as their role in the  
95 generation of plumes and hotspots (plume nurseries).

#### *3.1 Continuous Piles versus Plume Bundles*

96 The very first tomographic images of the Earth's lower mantle revealed the presence of a very long  
97 wavelength structure at the base of the mantle (degrees 2 and 3 in spherical harmonics expansion) anti-  
98 correlated with that observed in the gravity field (Dziewonski *et al.* 1977). The authors proposed two  
99 possible explanations for the unexpected sign of this correlation. The first is a dynamic interpretation in  
100 terms of thermal anomalies and core-mantle boundary (CMB) deflections due to mantle-wide convection;  
101 and the second involves lateral variations in composition due to the presence of eclogite-rich material in  
102 regions of past subduction and/or chemical plumes originating near the CMB. While these suggestions  
103 were quite speculative at the time, they are still actively pursued. The correlation, at large scale, of  
104 seismic structure in the deep mantle with anomalies in Earth's geoid and subduction zone configuration  
105 on the one hand (e.g. Hager *et al.* 1985; Dziewonski and Woodhouse 1987) and the distribution of  
106 hotspots and superswells on the other (Anderson 1982; Davies 1988; Richards *et al.* 1988; Richards and  
107 Engebretson 1992; Larson 1991a; Larson 1991b; McNutt 1998) was established soon thereafter.

108 Scores of seismic studies have since then confirmed the presence of LLSVPs and interpreted the  
109 seismically fast areas elsewhere as the remnants of the downgoing slabs from present and past subduction  
110 zones (Ricard *et al.* 1993; Lithgow-Bertelloni and Richards 1998), with a time-depth progressive

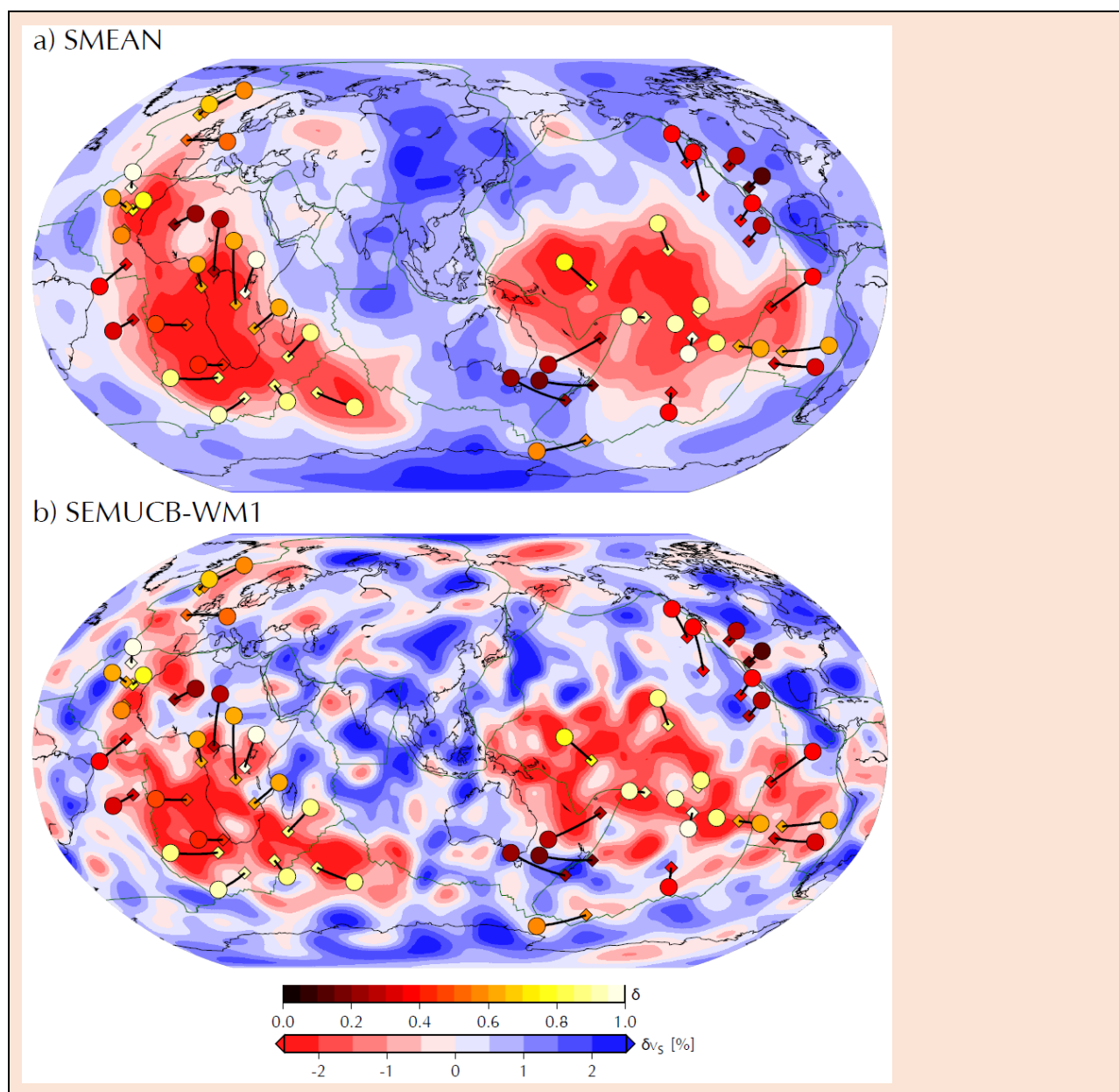
111 correlation demonstrated for the last 130 million years (Domeier *et al.* 2016). Recent tomographic models  
112 show considerable agreement on the extent of the LLSVPs and the shape of their borders when filtered up  
113 to spherical harmonics degree 16, or roughly 2,500 km wavelengths (Becker and Boschi 2002; Lekic *et*  
114 *al.* 2012). While the low seismic velocities within the LLSVPs indicate they are likely hot, the anti-  
115 correlation of bulk-sound and shear velocity within them (Su and Dziewonski 1997; Kennett *et al.* 1998;  
116 Masters *et al.* 2000) as well as the sharpness of their borders (e.g. Ni *et al.* 2002; Wang and Wen 2004;  
117 To *et al.* 2005) suggests that they may include a compositional and denser component, although the  
118 necessity of the latter has been questioned (Schuberth *et al.* 2009; Davies *et al.* 2012). If parts of the  
119 LLSVPs are denser than their surroundings (Ishii and Tromp 2004; Simmons *et al.* 2010) this would help  
120 resist entrainment in mantle convection and mixing with the overlying mantle and perhaps facilitate their  
121 survival over hundreds of millions of years (e.g. Mulyukova *et al.* 2015), and perhaps throughout most of  
122 Earth history, if they, at least partly represent primordial reservoirs (e.g. Ballmer *et al.* 2016). However,  
123 resolving the density structure in LLSVPs is challenging (Romanowicz 2001; Trampert *et al.* 2004) and  
124 different inferences on their effective density (Lau *et al.* 2017; Koelemeijer *et al.* 2017) might be due to  
125 thermal effects offsetting intrinsic density contrasts depending on the scale (e.g. McNamara 2019).

126         The distinct composition of LLSVPs could be due to the presence at the base of the mantle of a  
127 reservoir of primitive material, as might be suggested by studies that relate high  $^3\text{He}/^4\text{He}$  hotspots to  
128 plumes originating near the CMB (e.g. Macpherson *et al.* 1998; Williams *et al.* 2019; Mundl *et al.* 2017;  
129 Mundl-Petermeier *et al.* 2019; 2020) or to an accumulation of eclogite from subducted crust (e.g.  
130 Mulyukova *et al.* 2015), or some depth-dependent stratification of both (e.g. Ballmer *et al.* 2016). But it  
131 remains unclear whether the LLSVPs are compact, continuous piles of compositionally distinct material  
132 (e.g. McNamara and Zhong 2005; Steinberger and Torsvik 2012; Li and Zhong 2017) where mantle  
133 plumes are generated across their tops and along their edges, or whether LLSVPs represent two bundles  
134 of closely-spaced thermo-chemical plumes (Schubert *et al.* 2004; Davaille and Romanowicz 2020)  
135 separated by a ring of downwellings constrained by the geometry of tectonic plates at the surface (Zhang  
136 *et al.* 2010; Bull *et al.* 2014). This remains a subject of debate (e.g. Garnero *et al.* 2016; McNamara 2019;  
137 Heron *et al.* 2019; Davaille and Romanowicz 2020).

### 3.2 Mantle Plume Nurseries

138 Also debated are whether or not plumes in general, or those leading to LIPs, originate primarily along the  
139 edges of LLSVPs (Thorne *et al.* 2004; Boschi *et al.* 2007; Tan *et al.* 2011; Steinberger and Torsvik 2012;  
140 Davies *et al.* 2015a; Auzernmann *et al.* 2014; Hassan *et al.* 2015; Doubrovine *et al.* 2016). As the LLSVP  
141 edges are defined by sharp vertical and horizontal gradients in seismic shear-wave velocities (Ni *et al.*  
142 2002; To *et al.* 2005; Frost and Rost 2014) and plumes and reconstructed LIP locations tend to occur

143 close to vertically above them, they are proposed by some to act as ‘plume generation’ zones (**Figure 1b**)  
144 for all major hotspots and LIPs that have been active and remained approximately in place over at least  
145 the last 200 million years (Burke and Torsvik 2004; Torsvik *et al.* 2006; Burke *et al.* 2008). However, this  
146 is particularly difficult to determine in the case of the rather narrow African LLSVP (**Figure 2**).  
147 Interestingly, the roots of at least some of the LLSVP-rooted plumes do seem to contain unusually large  
148 ultra-low-velocity zones (ULVZs) (Hawaii: Cottaar and Romanowicz 2012; Samoa: Thorne *et al.* 2013;  
149 Iceland: Yuan and Romanowicz 2017; Marquesas: Kim *et al.* 2020) that are indicative of a  
150 compositionally different, likely denser component (Rost *et al.* 2005), possibly due to the presence of  
151 partial melt (Williams and Garnero 1996) or at least iron enrichment (Mao *et al.* 2006).



152

153 **Figure 2: Mantle Plume Locations and LLSVPs.** Global maps linking surface hotspots (circles) with  
154 depth-projected bottom source locations (diamonds) of mantle plumes (modified from Boschi *et al.*  
155 2007). Background coloring is shear wave anomaly at 2,875 km depth depicting where the two LLSVPs  
156 are located beneath Africa and the mid Pacific. The SMEAN composite (Becker and Boschi 2002) and  
157 SEMUCB-WM1 (French and Romanowicz 2014; 2015) models illustrate evolving tomographic views of  
158 the LLSVPs with the latter model supporting the view that LLSVPs are more granular, potentially  
159 indicating that LLSVPs are bundles of closely-spaced plumes instead of large piles. The maps suggest  
160 that most plumes originate above LLSVPs with a smaller group (Bowie, Cobb, Guadelupe and Socorro in  
161 the eastern Pacific) forming away from these lower mantle anomalous regions. The  $\delta$  metric in the upper  
162 color bar is used to color hotspots and inferred plume base locations; it is the normalized conduit length as  
163 identified in tomography where zero means that none and unity means that 100% of the plume length are  
164 mapped. The  $\delta_{v_s}$  in the lower color bar is the amplitude of the seismic shear velocity anomaly.

#### 4. Mantle Plume Characteristics

165 In this section, we review the key characteristics of mantle plumes. We will discuss how we know that  
166 plumes exist (imaging plumes) and what is the expected makeup and behavior of plume heads and tails  
167 (plume generation and ascent). From this a distinct picture emerges in which plumes are persistent  
168 features given the deep mantle conditions that occur in Earth today and, at least, over the last few  
169 hundreds of millions of years.

##### 4.1 Imaging Mantle Plumes

170 Where seismic tomography more easily picks up large-scale LLSVP superstructures and faster subducting  
171 slabs, imaging seismically slower ‘tubular’ mantle plumes in the ocean domain is challenging (Ritsema  
172 and Allen 2003; Sleep 2006). Within the framework of purely thermal convection with temperature-  
173 dependent viscosity in a fluid heated from below, a ‘thermal’ mantle plume conduit may only be 100-200  
174 km in diameter in the upper mantle but increase to more than 400 km in diameter in the lower half of the  
175 mantle that has a significantly higher viscosity (e.g. Steinberger and Antretter 2006). Plume detection is  
176 difficult because of a limited resolution in seismic tomography, especially due to a lack of earthquake  
177 sources and receiver stations in the ocean basins, and wavefront healing effects that hide low velocity  
178 domains of small diameter when classical travel time tomography is applied. The Iceland plume at first  
179 could only be seen in the upper mantle with an upwelling broader than expected (Wolfe *et al.* 1997; Allen  
180 *et al.* 2002). Similarly, imaging of the Hawaii plume originally resulted in the detection of a broad,  
181 inclined upwelling, disappearing from view below 1,500 km mantle depths (Montelli *et al.* 2004; Montelli  
182 *et al.* 2006; Wolfe *et al.* 2009). Generally, teleseismic travel time tomography has found plume-like

183 conduits of at least 400 km diameter in earlier studies (Nolet *et al.* 2005; Bijwaard and Spakman 1999). In  
184 more recent, higher resolution models, such broader plume-like conduits are found beneath many major  
185 hotspots, appear to be rooted near the CMB and rise all the way through the lower mantle, reaching upper  
186 mantle depths in the vicinity of hotspots (Boschi *et al.* 2008; French and Romanowicz 2015; Lei *et al.*  
187 2020). Their larger than ~500 km diameter (accounting for smearing due to the inversion process)  
188 indicates that they are likely thermochemical rather than purely thermal (French and Romanowicz 2015;  
189 Davaille *et al.* 2018) and most of these broad conduits are observed over the LLSVPs.

190         Anomalies in the travel times of seismic core waves, recorded by the dense USArray seismic  
191 network in North America, now also reveal a lower-mantle plume beneath the Yellowstone hotspot  
192 (Nelson and Grand 2018) that is probably unrelated to the Pacific LLSVP. This is a unique case study as  
193 Yellowstone is so far the only plume where the predicted tilted conduit shape can be matched in detail  
194 with a tomographic conduit image (Steinberger *et al.* 2019b). In the absence of individual conduits  
195 resolved at that time for most hotspots, Boschi *et al.* (2007) found that modeled plume conduits that take  
196 into account the effects of advection, and the associated displacement of plume sources at the base of the  
197 mantle, agree better with tomographic results than vertical conduits. The correlation of negative  
198 anomalies in seismic tomography with predicted plume conduits is indeed statistically highly significant  
199 (Boschi *et al.* 2008) and provides the counterpart to the correlation between mantle tomography and  
200 forward models of subduction (e.g. Steinberger *et al.* 2012). In addition, and different from  
201 geodynamically modelled conduits that tend to be tilted throughout the entire mantle (e.g. Steinberger  
202 2000; Steinberger and Antretter 2006), French and Romanowicz (2015) imaged plumes that are nearly  
203 vertical in much of the lower mantle, but some are strongly tilted above 1,000 km depth. This difference  
204 between geodynamic models and seismic observations should provide important constraints on mantle  
205 rheology. Such a strong tilt above ~1,000 km is also found for the Yellowstone plume (Nelson and Grand  
206 2018). This may indicate that current mantle flow models are overestimating overall flow speeds below  
207 ~1,000 km depth relative to rising speeds of plume heads and tails, and underestimating flow speeds  
208 above this horizon.

209         Recent global seismic tomography indicates that both downgoing slabs (e.g. Fukao and Obayashi  
210 2013) and upwellings, as manifested by broad plume conduits (e.g. French and Romanowicz 2015; Lei *et al.*  
211 2020) appear to be deflected horizontally not only around 660 km depth—where we know there is a  
212 seismic discontinuity that corresponds to the phase transition from ringwoodite to bridgmanite and  
213 oxides—but also around 1,000 km depth. This is accompanied by a decorrelation between the longest  
214 wavelength seismic structures in the extended transition zone (400-1,000 km) and the deeper mantle (e.g.  
215 Rudolph *et al.* 2015), which is visible even in lower resolution seismic mantle models and indicated by  
216 seismic data suggesting vertical decorrelation at ~800 km depth (Boschi and Becker 2011). This implies a

217 change of material properties that may not coincide with the 660 km discontinuity, and could be  
218 explained by an increase in mantle viscosity somewhat deeper than traditionally considered, given the  
219 rather non-unique constraints provided by geoid and post-glacial rebound data (e.g. King and Masters  
220 1992; Mitrovica and Forte 2004).

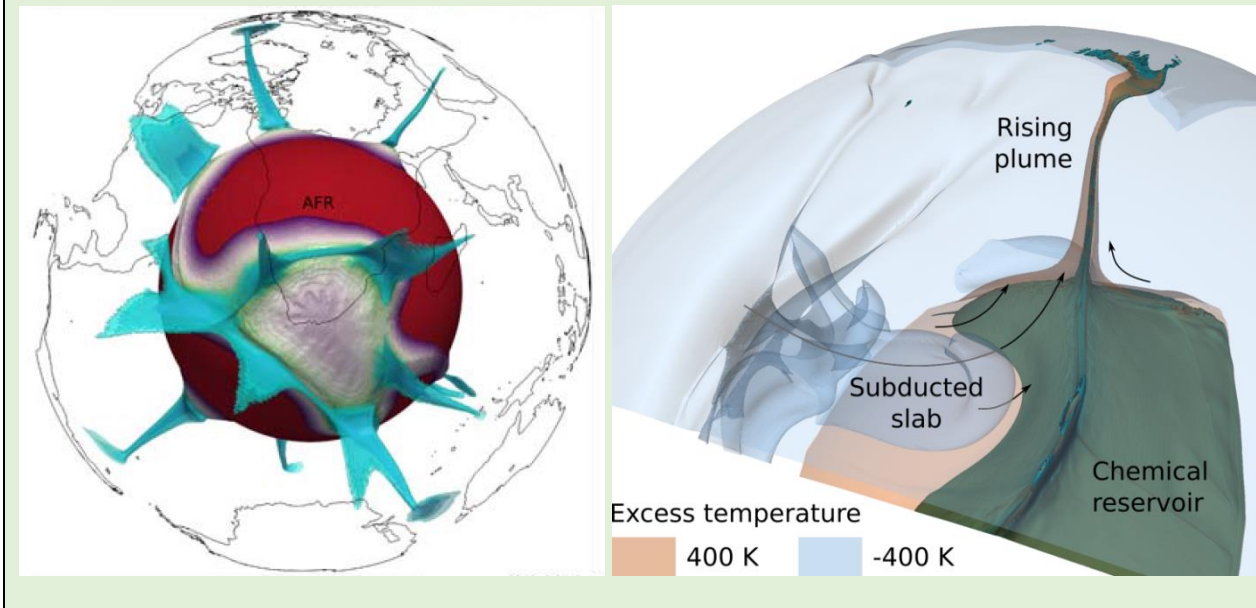
221 In summary, while there is still progress to be made in resolving the details of plume-like  
222 conduits, and in particular their actual diameter, seismic tomography has already shown the presence of  
223 mantle plumes below major hotspots, rooted at the core-mantle boundary, although the roots are generally  
224 shifted horizontally from the location of the corresponding hotspots due to plume conduit tilting in the  
225 upper third of the mantle. Most importantly, they are typically not the simple, purely thermal plumes that  
226 geophysicists have been hunting for. Such classical thermal plumes with narrow tails ~200 km in  
227 diameter (Farnetani 1997) but possibly reaching ~400 km in parts of the lower mantle are not ruled out,  
228 but they are probably mostly below the resolution of current global seismic tomography. Moreover, the  
229 broad plumes currently detected do not rise vertically from the CMB to the corresponding hotspot, they  
230 show significant deflections in primarily the upper 1,000 km of the mantle, likely due to mantle wind as  
231 predicted by geodynamic computations (Steinberger and O’Connell 1998; Steinberger 2000).

#### 4.2 Models of Plume Generation and Ascent

232 Localized hot upwelling plumes are expected in any terrestrial-type planet mantle, where convection  
233 operates with some amount of bottom heating, or where other domains with concentrated heat production  
234 can sustain a thermal boundary layer (**Box 1**). Differences in temperature and/or composition will cause  
235 variations in density that may result in thermochemical instabilities near boundary layers as the beginning  
236 of an upwelling and, when it persists, a rising mantle plume (e.g. Jellinek and Manga 2004).

237 **Box 1: Dynamic Simulations of Plume Behavior in ‘Earth-like’ Planets.** Although thermal instabilities  
238 at the core-mantle boundary are inevitable, conditions in Earth’s mantle are such that they cannot grow  
239 undisturbed. Rather, mantle flow driven by slabs, many of which are subducted to the deep lower mantle  
240 and piled up into ‘slab graveyards’ (Ricard *et al.* 1993; Lithgow-Bertelloni and Richards 1998;  
241 Steinberger *et al.* 2012; Mulyukova *et al.* 2015; van der Meer *et al.* 2018; Domeier *et al.* 2016) will  
242 trigger plumes, characteristically above Large Low Shear Velocity Provinces (LLSVP) and along their  
243 edges (Tan *et al.* 2002; Steinberger and Torsvik 2012; Hassan *et al.* 2015; Li and Zhong 2017). The left-  
244 hand panel shows the results of a 3D and time-dependent numerical model with plumes (blue) rising from  
245 a LLSVP situated below southern Africa (Hassan *et al.* 2015). Rising from LLSVP margins, plumes in  
246 this model are significantly hotter than surrounding mantle, starting out with large temperature anomalies  
247 of about 500° K in the lowermost mantle, as shown in the right-hand panel (Dannberg and Gassmüller

248 2018). The plumes will slowly cool down when they rise, with smaller plumes losing a larger fraction of  
249 their heat on the way up through the mantle. However, larger plumes will retain their heat better (Albers  
250 and Christensen 1996; Zhong 2006; Leng and Zhong 2008) with estimated excess plume temperatures of  
251 200-300 °K at asthenospheric depths for Hawaii (Moore *et al.* 1998; Ribe and Christensen 1999; Schubert  
252 *et al.* 2001).

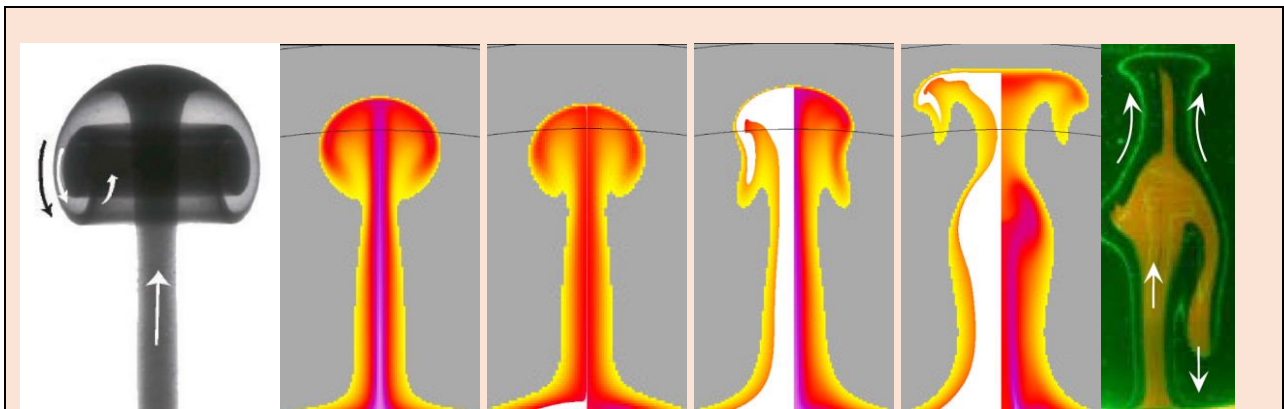


253

254 Typical ‘thermal’ mantle plumes in Earth will have a broad plume head, up to roughly thousand  
255 kilometers in diameter, followed by a narrow plume tail, not wider than a couple of hundred kilometers  
256 (e.g. Richards *et al.* 1989; Sleep 1990; Coffin and Eldholm 1994; Davaille 1999; Campbell 2007). These  
257 plumes can persist over long geological times, but only if the thermal boundary layer from which they  
258 arise is also maintained for hundreds of millions of years (Sleep 2003; Tan *et al.* 2002; Jellinek and  
259 Manga 2004; Burke *et al.* 2008). In fact, for plumes to keep rising through the entire mantle, a lower limit  
260 of ~500-1000 kg/s of anomalous mass flux is required to sustain the plume tails (Albers and Christensen  
261 1996). Rising plumes from near the LLSVPs are expected to be buoyant due to their hotter temperatures,  
262 but if they entrain chemically distinct materials from the LLSVPs that are heavier than surrounding  
263 mantle (Lau *et al.* 2017) then their buoyancies may be substantially reduced (Lin and van Keken 2006a;  
264 Mulyukova *et al.* 2015). The anomalous density of LLSVPs (Lau *et al.* 2017; Koelemeijer *et al.* 2017)  
265 and the nature of the entrainment of other materials during plume ascent (e.g. Farnetani 1997; McNamara  
266 and Zhong 2004) are still debated. Because of time-dependent and variable amounts of entrainment,  
267 highly complex plume behavior and shapes (Figure 3) may result that substantially differ from the  
268 classical head-and-tail structure (Farnetani and Samuel 2005; Lin and van Keken 2006b; Kumagai *et al.*  
269 2008). For example, negative buoyancy of (denser) material entrained from LLSVPs in plume heads may

270 cause material to sink back into the ascending plume (Ballmer *et al.* 2013; Dannberg and Sobolev 2015)  
271 leading to broader plume conduits that are a few hundred kilometers wider than typical thermal plumes.

272 How long it takes for a plume head to traverse the mantle after forming at the core-mantle  
273 boundary is difficult to estimate. It primarily depends on its buoyancy, arising from a density contrast of  
274 about  $30 \text{ kg/m}^3$  for thermal plumes, but which could be much less for thermochemical plumes, and the  
275 average viscosity of the surrounding mantle. Widely discrepant estimates exist for mantle viscosity, as it  
276 may be (locally) controlled by variations in temperature and stress that may render global average  
277 viscosity estimates not applicable for plumes (e.g. Larsen and Yuen 1997). One traversal time estimate  
278 can be made because reconstructed LIP eruptions are correlated with LLSVP margins and therefore LIPs  
279 are hypothesized to erupt from those margins. But in order for that correlation to be maintained during  
280 their rise through the mantle, plume heads must rise up from the lower mantle rather fast, probably within  
281 30 million year or less, to avoid large lateral deflections, consistent with numerical models (e.g. Hassan *et al.*  
282 *et al.* 2015). However, for smaller plume heads, such as for the Yellowstone plume—which is not associated  
283 with the Pacific LLSVP and is located in a region dominated by subduction—it is estimated that its plume  
284 head rose more slowly, taking 80 million years or longer (Steinberger *et al.* 2019b). Plumes rise therefore  
285 considerably faster than slab sink, at estimated speeds of 1-2 cm/yr, such that slabs require  $\sim 150\text{-}200$   
286 million years to reach the bottom of the mantle (Steinberger *et al.* 2012; Hassan *et al.* 2015; Butterworth  
287 *et al.* 2014; Van der Meer *et al.* 2018). In addition, during ascent, the even more slowly rising plume  
288 conduits are predicted to become increasingly tilted with time, as their roots become shifted towards  
289 large-scale upwellings, likely above the two LLSVPs (Steinberger and O’Connell 1998; Steinberger  
290 2000).



291  
292 **Figure 3: A Gallery of Rising Thermal and Thermochemical Plumes.** From left to right: Laboratory  
293 model of rising thermal plume head, connected by a stem to the source region (Campbell *et al.* 1989);  
294 four numerical models of one axisymmetric thermal and three thermochemical plumes (Lin and van  
295 Keken 2006a) with colors representing temperature (magenta=hottest; yellow=coolest) and entrained  
296 material (white) with variable chemical excess densities of 200, 50 and 60 (from left to right)  $\text{kg/m}^3$  in left

297 half of the visualized plume conduits; and a laboratory syrup tank model of a plume that partially fails  
298 when entrained materials (that are too heavy) collapse in the top of the conduit (Kumagai *et al.* 2008).

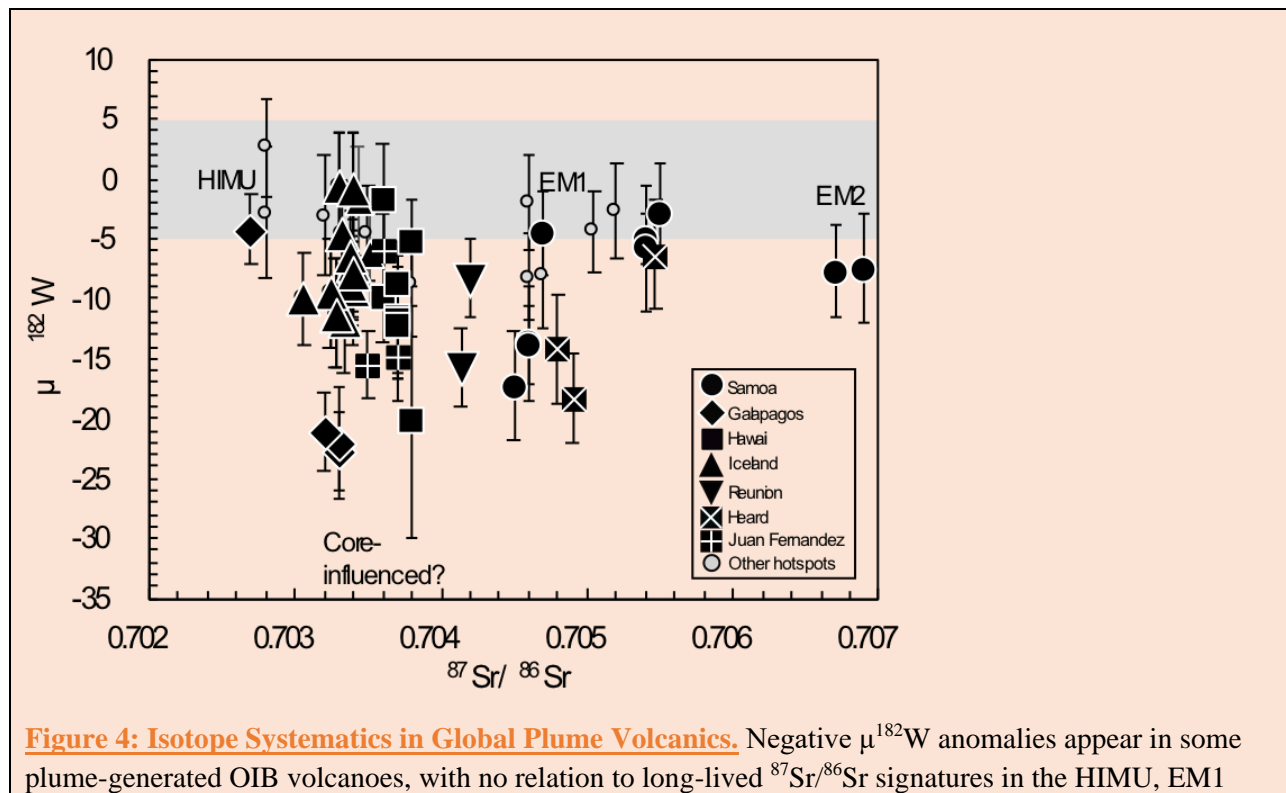
299           Eventually, when the plume head reaches the lithosphere, a LIP may form over short amounts of  
300 geological time, likely in less than a million years (Coffin and Eldhom 1994). Long-lived hotspot tracks  
301 may form after that and persist in some cases for 80 to 120 million years (Peate 1997; Koppers *et al.*  
302 2012; Konrad *et al.* 2018a) or even longer (e.g. Hoernle *et al.* 2015). Several hotspot tracks are associated  
303 with flood basalts at one end (e.g. Tristan, Reunion) and thus may correspond to typical thermal plumes  
304 with a tail following the head (Richards *et al.* 1989; Ernst and Buchan 2003). Although the typical  
305 lifetime of a deep mantle plume is likely long, on the order of ~100 million years, some of the older  
306 Pacific hotspot tracks were only active in the Cretaceous and do not correspond to any currently active  
307 hotspot (e.g. Hess and Shatsky Rise; Koppers *et al.* 2001; Tejada *et al.* 2016). Evidence from the  
308 bathymetric record in the Pacific Ocean also indicates that many hotspot trails are characterized by  
309 shorter seamount trails, apparently only active for up to 30 million years (Clouard and Bonneville 2001;  
310 Koppers *et al.* 2003). These surface expressions, however, do not have to mean that the mantle sources  
311 are short-lived per se, but rather that instabilities may develop in rising mantle plumes, for example, once  
312 conduits are tilted more than 60° from the vertical, at which stage they may break apart (Whitehead 1982;  
313 Steinberger and O’Connell 1998). Plumes may also go extinct if their buoyancy fluxes are too high and  
314 they cut themselves off from a supply of hot mantle material. Plumes may become internally unstable and  
315 collapse due to insufficient buoyancy, they may appear to switch on/off if rising plumes are pulsating or  
316 boudinaging, and in some cases they may begin without flood basalts. All possible explanations for such  
317 intermittent plume behaviors and plumes without heads are still being mapped out and debated.

## 5. Mantle Plumes Illuminating Deep Mantle Heterogeneities

318 Plumes provide a unique view into Earth’s mantle, revealing its intricate chemical makeup and evolution  
319 over billions of years. Although seamount trails and LIPs have complex construction histories, variations  
320 in their chemical compositions provide clues about early Earth (enduring ancient signatures) and the  
321 number and composition of distinct chemical endmembers that reside in Earth’s interior (mantle  
322 heterogeneities). These clues lead to intriguing debates on how deep, and at what length and time scales,  
323 those endmembers are manifested in the mantle (location of primordial and recycled reservoirs) and how  
324 hotspot trails may ‘mimic’ these heterogeneities (striped plumes).

### 5.1 Enduring Ancient Signatures

325 Extinct short-lived isotope systems (such as  $^{129}\text{I}$ - $^{129}\text{Xe}$  [with a half-life of  $t_{1/2}=15.7$  Ma],  $^{182}\text{Hf}$ - $^{182}\text{W}$   
 326 [ $t_{1/2}=8.9$  Ma] and  $^{146}\text{Sm}$ - $^{142}\text{Nd}$  [ $t_{1/2}=103$  Ma]) provide unmatched insights in the processes happening in  
 327 the earliest approximately 50 (for  $^{182}\text{W}$ ) to 500 million years (for  $^{142}\text{Nd}$ ) of Earth's history (Halliday 2004;  
 328 Carlson and Boyet 2009; Mundl *et al.* 2017; Mukhopadhyay and Parai 2019). Because radioactive decay  
 329 in these isotope systems is rather rapid on planetary timescales, resolvable changes in these isotopic  
 330 systems ( $^{129}\text{Xe}/^{130}\text{Xe}$ ,  $^{182}\text{W}/^{184}\text{W}$  and  $^{142}\text{Nd}/^{144}\text{Nd}$ ) are restricted to the Hadean, the opening eon in Earth's  
 331 history, ending 4 billion years ago. The presence of such ancient isotopic anomalies in mantle plume  
 332 source regions, therefore, suggest that some primordial mantle reservoirs are still present in the Earth's  
 333 interior despite extensive convective mixing (Mukhopadhyay 2012; Peters *et al.* 2018; Williams *et al.*  
 334 2019; Mundl-Petermeier *et al.* 2020). For example, the  $^{129}\text{I}$ - $^{129}\text{Xe}$  system shows a marked difference in  
 335  $^{129}\text{Xe}/^{130}\text{Xe}$  between Earth's mantle and atmosphere (Allegre *et al.* 1983), and heterogeneous  $^{129}\text{Xe}/^{130}\text{Xe}$   
 336 is also preserved in the mantle since the Hadean (Mukhopadhyay 2012). Application of the  $^{182}\text{Hf}$ - $^{182}\text{W}$   
 337 and  $^{146}\text{Sm}$ - $^{142}\text{Nd}$  systems confirms the survival of Hadean-generated signatures in the modern mantle,  
 338 with resolvable  $^{182}\text{W}$  and  $^{142}\text{Nd}$  anomalies in OIB present in mantle plumes (Mundl *et al.* 2017; Peters *et*  
 339 *al.* 2018; Horan *et al.* 2018), but the discovery of anomalous  $^{182}\text{W}$  in plume-head-generated flood basalts  
 340 (Rizo *et al.* 2016) remains controversial (Kruijer and Kleine 2018).



344 and EM2 mantle sources. One interpretation of these observations is that that some deeply sourced mantle  
345 plumes with strongly negative  $\mu^{182}\text{W}$  anomalies have inherited a W-isotopic signature of Earth's core  
346 (Rizo *et al.* 2019; Mundl-Petermeier *et al.* 2020). In this diagram the grey bar represents the  $2\sigma$   
347 reproducibility of the standard. Estimated core  $\mu^{182}\text{W}$  is -220 (Touboul *et al.* 2012).

348 More recent work, however, established that  $^{182}\text{W}$  anomalies in plume-formed OIB do not exhibit  
349 straightforward relationships (**Figure 4**) with long-lived heavy radiogenic isotopes, such as  $^{87}\text{Sr}/^{86}\text{Sr}$  ( $t_{1/2} =$   
350 49 billion years). Instead, most OIB that host negative  $^{182}\text{W}$  anomalies also appear to be associated with  
351 high  $^3\text{He}/^4\text{He}$  lavas (Mundl *et al.* 2017; Mundl-Petermeier *et al.* 2019; 2020) that in turn are typically  
352 interpreted to sample deep primordial mantle signatures (e.g. Kurz *et al.* 1982) present in only the hottest  
353 and most buoyant plumes (Jackson *et al.* 2017). It is hypothesized that these OIB  $^{182}\text{W}$  anomalies reflect a  
354 contribution from Earth's core, which has preserved a low  $\mu^{182}\text{W}$  value (the deviation of  $^{182}\text{W}/^{184}\text{W}$  from  
355 the terrestrial standard in parts per million) because tungsten is a moderately siderophile element that,  
356 during core formation, became enriched in the Earth's core relative to the short-lived, lithophile  
357 radioactive parent ( $^{182}\text{Hf}$ ), which remained in the mantle (Rizo *et al.* 2019; Mundl-Petermeier *et al.* 2020).  
358 It is possible that this core material is partitioned back into the mantle at the base of mantle plumes, aided  
359 by silicate melting (Mundl-Petermeier *et al.* 2020), possibly in the ultra-low seismic velocity zones at the  
360 core-mantle boundary (**Figure 1b**).

## 5.2 Mantle Heterogeneities Inferred from Hotspots

361 Lower-mass stable isotopes (such as oxygen, sulfur, calcium, and iron) provide distinguishing 'surface'  
362 isotopic signatures because low temperature alteration, biological processes, and other shallow-level  
363 mechanisms modify their isotopic ratios. The discovery of these 'surficial' signatures in mantle plume  
364 source regions, therefore, provides first order evidence that Earth is recycling its lithospheric plates in  
365 subduction zones at a global scale and is resupplying the deep source regions of mantle plumes with  
366 various 'crustal' materials (Eiler *et al.* 1996; Huang *et al.* 2011a; Cabral *et al.* 2013; Konter *et al.* 2016;  
367 Nebel *et al.* 2019; Gleeson *et al.* 2020). High-mass radiogenic isotopes (such as  $^{87}\text{Sr}/^{86}\text{Sr}$ ,  $^{143}\text{Nd}/^{144}\text{Nd}$ ,  
368  $^{206}\text{Pb}/^{204}\text{Pb}$  and  $^{176}\text{Hf}/^{177}\text{Hf}$ ) paint an even more complex picture of global mantle heterogeneity, providing  
369 insight into which, how many, and in what way mantle end members are involved in the chemical  
370 dynamics of mantle plume formation (Allegre 1982; Hofmann and White 1982; Zindler and Hart 1986;  
371 White 2010; Jackson *et al.* 2018b). Many of the global hotspot systems have two, three, or more, distinct  
372 components in their mantle plume source regions (Harpp and White 2001; Hoernle *et al.* 2000; Jackson *et*  
373 *al.* 2014).

374 Lava flows from LIPs and hotspot-related OIBs thus sample a diverse array of long-lived  
375 radiogenic isotopic compositions. These chemical trends have been classified into four primary "species"

376 or endmembers (**Figure 4**) based on isotopic composition: **EM1** (enriched mantle I) characterized by low  
377 moderately-high  $^{87}\text{Sr}/^{86}\text{Sr}$  and low  $^{206}\text{Pb}/^{204}\text{Pb}$ ; **EM2** (enriched mantle II) characterized by high  $^{87}\text{Sr}/^{86}\text{Sr}$   
378 and intermediate  $^{206}\text{Pb}/^{204}\text{Pb}$ ; **HIMU** (or high “ $\mu$ ”, where  $\mu = ^{238}\text{U}/^{204}\text{Pb}$ ) with low  $^{87}\text{Sr}/^{86}\text{Sr}$  and high  
379  $^{206}\text{Pb}/^{204}\text{Pb}$ ; and a geochemically-depleted component variously referred to as **PREMA** (Prevalent  
380 Mantle; Zindler and Hart 1986), **FOZO** (Focus Zone; Hart *et al.* 1992), or **C** (Common; Hanan and  
381 Graham 1996).

382         The EM2 mantle domain almost certainly relates to recycling of terrigenous sediments derived  
383 from ancient upper continental crust, and is manifested mostly clearly in Samoan hotspot lavas (Jackson  
384 *et al.* 2007; Workman *et al.* 2008), where the lavas exhibit clear radiogenic isotopic and trace element  
385 signature fingerprints seen only in continental crust. There is less certainty about the origin of the HIMU  
386 component in hotspots, defined by their highly radiogenic  $^{206}\text{Pb}/^{204}\text{Pb}$ , a signature that has been attributed  
387 to sampling of ancient subducted oceanic crust (Hofmann and White 1982) or marine carbonates (Castillo  
388 2015), metasomatism of the underlying oceanic lithospheric mantle (Pilet *et al.* 2008) or the  
389 subcontinental lithospheric mantle (Weiss *et al.* 2016), and possibly could originate from a reservoir in  
390 the transition zone (Nebel *et al.* 2013; Mazza *et al.* 2019; Huang *et al.* 2020) or lower mantle (Collerson  
391 *et al.* 2010). The presence of mass independently fractionated sulfur (MIF-S) isotopes in endmember  
392 HIMU lavas from Mangaia Island supports an oceanic crustal recycling model (Cabral *et al.* 2013) as  
393 these MIF-S are interpreted to represent a unique fingerprint from Archean atmosphere that become  
394 associated with oceanic crust (Farquhar *et al.* 2002). The origin of EM1 lavas is the least certain among  
395 the mantle domains, as both deep and shallow mantle metasomatic processes have been invoked, as well  
396 as recycling of a variety of different lithospheric protoliths (see Garapic *et al.* 2015 and references  
397 therein). However, the discovery of MIF-S in EM1 lavas from Pitcairn supports models advocating  
398 recycling of shallow crustal protoliths (Delavault *et al.* 2016), and radiogenic isotopic and trace element  
399 signatures are consistent with a continental crustal protolith in the EM1 mantle (Eisele *et al.* 2002).

400         Nonetheless, extreme EM1-EM2 and HIMU compositions are relatively uncommon: the bulk of  
401 volcanism at hotspots and oceanic LIPs (Zindler and Hart 1986) is geochemically depleted relative to a  
402 chondrite-based bulk silicate Earth—the long-accepted compositional model for the formation of our  
403 planet (McDonough and Sun 1995). This suggests that, like the upper mantle, the lower mantle also must  
404 have experienced a strong depletion of incompatible elements by ancient prolonged crustal extraction  
405 (Hart *et al.* 1992). Consistent with this observation, studies based on the short-lived  $^{146}\text{Sm}$ - $^{142}\text{Nd}$  system  
406 suggested that the accessible silicate Earth has elevated  $^{142}\text{Nd}/^{144}\text{Nd}$  and is the product of a global early-  
407 Hadean mantle depletion event (Boyet and Carlson, 2005; Jackson *et al.* 2010; Caro and Bourdon, 2010).  
408 This model requires a complementary early-formed enriched reservoir (now hidden) with low  $^{142}\text{Nd}/^{144}\text{Nd}$   
409 that resides in the deep mantle or was lost to space (Jellinek and Jackson 2015; and references therein).

410 While this model was questioned (Bouvier and Boyet 2016; Burkhardt *et al.* 2016) more recent work may  
411 support a non-chondritic composition for the silicate Earth caused by a massive Hadean depletion event  
412 (Debaille *et al.* 2019). In this debate geoneutrinos present an opportunity to map out the spatial  
413 distribution of geochemical reservoirs in the Earth's deep interior, particularly with respect to the  
414 geochemically-important radioactive heat-producing elements (U, Th, K), which would be elevated in a  
415 putative hidden early enriched reservoir. This mapping of geoneutrinos may help resolve the debate over  
416 the bulk composition of the planet (Šrámek *et al.* 2013).

### 5.3 Location of Primordial and Recycled Reservoirs

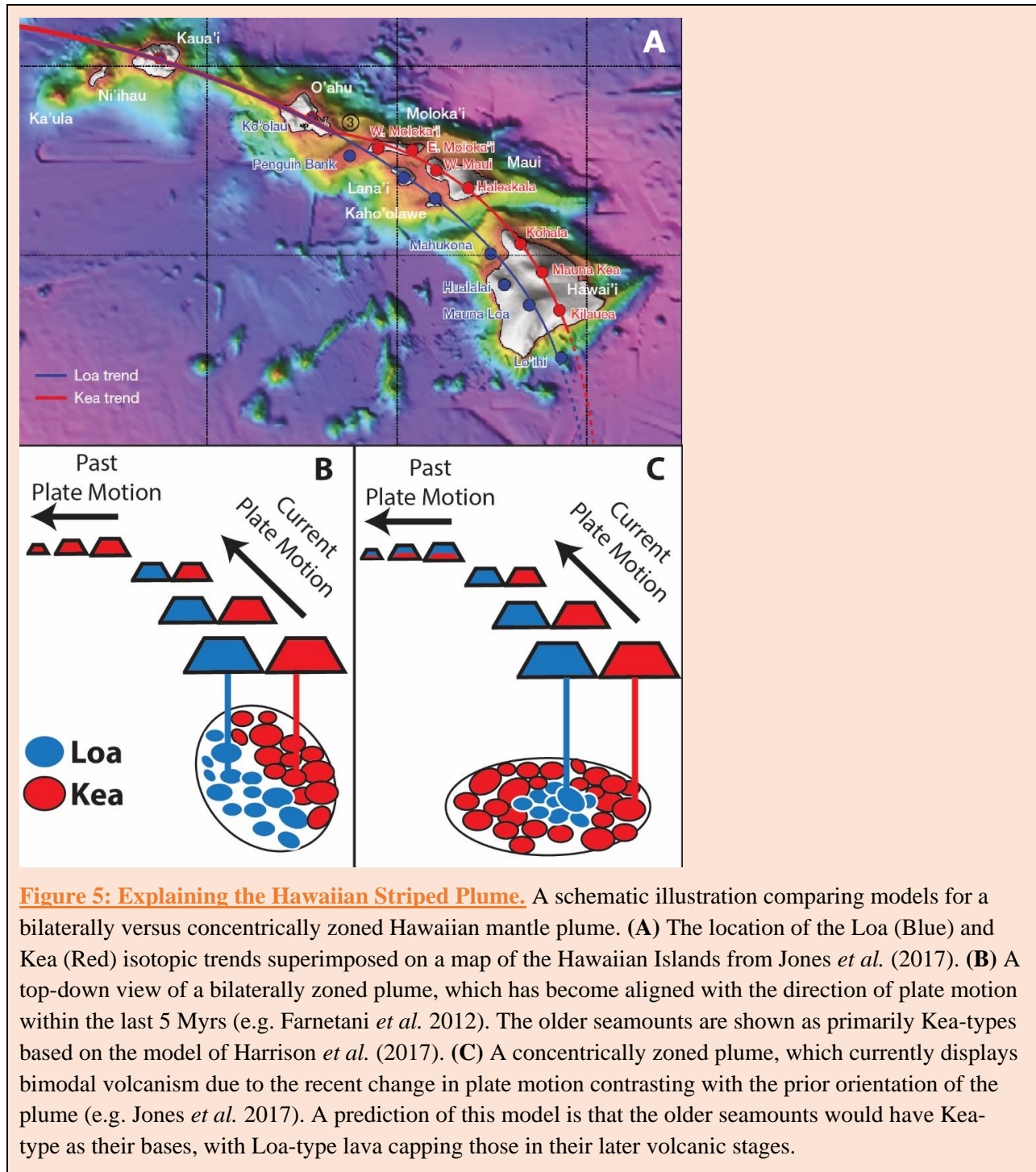
417 Mechanisms for the long-term preservation of the Hadean geochemical anomalies are imperfectly  
418 understood (Gülcher *et al.* 2020), but storage in dense, viscous domains of the deep mantle may isolate  
419 Hadean-formed reservoirs from convective motions of the mantle (Samuel and Farnetani 2003; Lin and  
420 van Keken 2006a; Deschamps *et al.* 2011). The two LLSVP regions at the core-mantle boundary are  
421 attractive locations in this regard (e.g. Tackley 1998; Macpherson *et al.* 1998; Mukhopadhyay 2012),  
422 though alternatives have been suggested (e.g. Allegre *et al.* 1984; Becker *et al.* 1999; Ballmer *et al.*  
423 2017). Hotspots with the highest (most primordial)  $^3\text{He}/^4\text{He}$  ratios do appear to be positioned over the  
424 LLSVPs (Macpherson *et al.* 1998; Garapic *et al.* 2015; Williams *et al.* 2019) and are consistent with an  
425 ancient source for these seismic features. However, to date  $^{129}\text{Xe}$ ,  $^{142}\text{Nd}$ , and  $^{182}\text{W}$  OIB short-lived isotope  
426 datasets are still statistically too small to conclusively link the Hadean isotopic anomalies to the LLSVPs.  
427 Much larger Sr-Nd-Pb isotope datasets confirm that EM1-EM2 hotspots are geographically linked to both  
428 of the LLSVPs (Castillo 1988; Jackson *et al.* 2018a). However, a recent study suggests that only the  
429 Atlantic LLSVP hosts EM signatures (Doucet *et al.* 2020), but such arguments hinge on the selection of  
430 plumes (e.g. Jackson *et al.* 2018a) and more work is needed to better identify reservoir geometries and  
431 dynamics. HIMU hotspots seemingly are not linked to the LLSVPs (Jackson *et al.* 2018b), leaving the  
432 location of this scarce domain uncertain. In fact, the EM and HIMU domains appear to be spatially  
433 decoupled in Earth's mantle, which is unexpected given that both likely formed following subduction and  
434 recycling as part of the plate tectonic cycle (Jackson *et al.* 2018b).

435 While the ULVZs are argued to be compositionally distinct (Li *et al.* 2017) it is not yet possible  
436 to evaluate whether ULVZs sample geochemical reservoirs different from LLSVPs. Where some plume  
437 conduits are clearly associated with ULVZs (Cottaar and Romanowicz 2012; Thorne *et al.* 2013; Yuan  
438 and Romanowicz 2017; Kim *et al.* 2020), other plumes may not be (or, they are, but the ULVZs have not  
439 yet been seismically imaged at their plume roots). Until the distribution of ULVZs has been  
440 conclusively “mapped out” it will not possible to determine whether ULVZ-related plumes have a  
441 different composition than plumes that are not, and this currently limits what can be inferred about the

442 isotope geochemistry of the ULVZs. Ultimately, the evolutions of these geochemical reservoir are linked  
443 to plate tectonic processes, including recycling of oceanic and continental crust and transport by plumes,  
444 and these processes control the composition, location, size, and longevity of geochemical reservoirs in the  
445 Earth's interior.

#### 5.4 Striped Plume Expressions

446 Surface expressions of plume-fed volcanism in the oceanic realm are highly varied and complex. A most  
447 notable complexity is the formation of 'double' track volcanic hotspot trails that are geochemically  
448 'striped' over millions of years of plume history. These kind of surface expressions may be governed by  
449 the makeup of the plumes themselves (Abouchami *et al.* 2005; Farnetani and Hofmann 2010; Huang *et al.*  
450 2011b; Weis *et al.* 2011; Hofmann and Farnetani 2013; Hoernle *et al.* 2015; Dannberg and Gassmüller  
451 2018), and by their interactions with the overriding tectonic plates and any changes in plate motion and  
452 direction (Moore *et al.* 1998; Hieronymus and Bercovici 1999; Davies *et al.* 2015b; Jones *et al.* 2017).  
453 The presence of these geochemically-resolved dual volcanic trends in ocean island systems was first  
454 noticed for the Hawaiian Islands by Tatsumoto (1978) and follow the 'Loa' and 'Kea' volcanic tracks  
455 (Figure 5a) as described by Dana (1849). Since then, *en echelon* trends have also been observed for the  
456 Easter, Foundation, Galapagos, Marquesas, Samoan, Society, Tristan-Gough and Rurutu hotspot tracks  
457 (Hoernle *et al.* 2000, 2015; Werner *et al.* 2003; Huang *et al.* 2011b; Payne *et al.* 2013; Harpp *et al.* 2014;  
458 Chauvel *et al.* 2012; Koppers *et al.* 2011a; Finlayson *et al.* 2019).



459  
 460 **Figure 5: Explaining the Hawaiian Striped Plume.** A schematic illustration comparing models for a  
 461 bilaterally versus concentrically zoned Hawaiian mantle plume. (A) The location of the Loa (Blue) and  
 462 Kea (Red) isotopic trends superimposed on a map of the Hawaiian Islands from Jones *et al.* (2017). (B)  
 463 A top-down view of a bilaterally zoned plume, which has become aligned with the direction of plate motion  
 464 within the last 5 Myrs (e.g. Farnetani *et al.* 2012). The older seamounts are shown as primarily Kea-types  
 465 based on the model of Harrison *et al.* (2017). (C) A concentrically zoned plume, which currently displays  
 466 bimodal volcanism due to the recent change in plate motion contrasting with the prior orientation of the  
 467 plume (e.g. Jones *et al.* 2017). A prediction of this model is that the older seamounts would have Kea-  
 468 type as their bases, with Loa-type lava capping those in their later volcanic stages.

469 There are currently two debated models on the origin of these dual isotopic signatures and the  
 470 inferred chemical structure of mantle plumes: the bilaterally zoned plume (Abouchami *et al.* 2005;  
 471 Farnetani and Hofmann 2010; Huang *et al.* 2011b, Weis *et al.* 2011; Hoernle *et al.* 2015; Chauvel *et al.*  
 472 2012; Dannberg and Gasmöller 2018) and concentrically zoned plume model (Frey and Rhodes, 1996;  
 473 Kurz *et al.* 1996; DePaolo *et al.* 2001; Jones *et al.* 2017; Konrad *et al.* 2018b). The bilaterally zoned

474 plume model postulates that the geochemical stripes observed among most ocean island chains originate  
475 from a mantle plume structure that is divided into two distinct chemical reservoirs (**Figure 5b**). The  
476 plume could contain a bilaterally continuous structure (Hofmann and Farnetani 2013), two zones  
477 consisting of vertically continuous filaments with some spacing in-between (Abouchami *et al.* 2005), or a  
478 partly ordered structure with some mixing between the zones (Ren *et al.* 2005). As some mantle plumes  
479 appear to be rooted on the boundary between LLSVPs and ambient lower mantle, it is possible that  
480 bilaterally zoned plumes sample both LLSVP ( $\pm$  ULVZ) and the ambient lower mantle materials (Huang  
481 *et al.* 2011b; Weis *et al.* 2011; Hofmann and Farnetani 2013).

482 In the bilaterally zoned plume model for Hawaii, the southern ‘Loa’ component (EM1) of the  
483 Hawaiian plume would represent incorporation of LLSVP material, while the northern ‘Kea’ component  
484 (PREMA) would represent ambient lower mantle (Weis *et al.* 2011). However, to explain the general  
485 absence of a Loa component in the Hawaiian plume prior to ~5 million years ago, Harrison *et al.* (2017)  
486 argue that the LLSVP-derived Loa component only became entrained in the plume conduit intermittently  
487 between ~47 and 6.5 Ma, and then consistently from 6.5 Ma to the present day. Similar geographical and  
488 temporal trends are seen within the Marquesas and Samoan Islands (Huang *et al.* 2011b; Chauvel *et al.*  
489 2012), showing the potential ability to link surficial geochemical signatures to the lowermost mantle  
490 geophysical domains.

491 The concentrically zoned plume model argues that plumes concentrate the hottest and densest  
492 materials in their centers (**Figure 5c**) during ascent from the core-mantle boundary (Jones *et al.* 2016).  
493 This model explains surficial isotopic stripes as being derived from sampling of the plume core versus its  
494 outer rim (DePaolo *et al.* 2001). The concentric model has been supported by noble gas studies that  
495 indicate that the most chemically ‘primitive’ lava flows with high  $^3\text{He}/^4\text{He}$  ratios are typically found  
496 within the central regions of ocean islands (Kurz *et al.* 1996; DePaolo *et al.* 2001; Konrad *et al.* 2018b).  
497 An alternative concentric plume model argues for the melting of differing lithologies at differential depths  
498 in the plume as a function of plume-plate interaction (Jones *et al.* 2017). However, an unrelated (and  
499 controversial) change in Pacific plate motion at ~2.5 Ma is required to force a depth shift in mantle  
500 melting that initially would have produced Kea-type lava flows (from a deeper peridotite melting region)  
501 followed by Loa-type lava flows (from a shallow pyroxenite source) after the plate motion change (Jones  
502 *et al.* 2017). This model currently does not explain the complex zonation patterns observed along the  
503 Tristan-Gough track on the African plate (Hoernle *et al.* 2015).

## 6. Mantle Plumes and Plate Tectonics

504 Understanding if and why certain plumes move, in which directions, in unison or not, and how fast, is an  
505 ongoing debate. In this section, we show that plumes can move independently and at speeds typically less

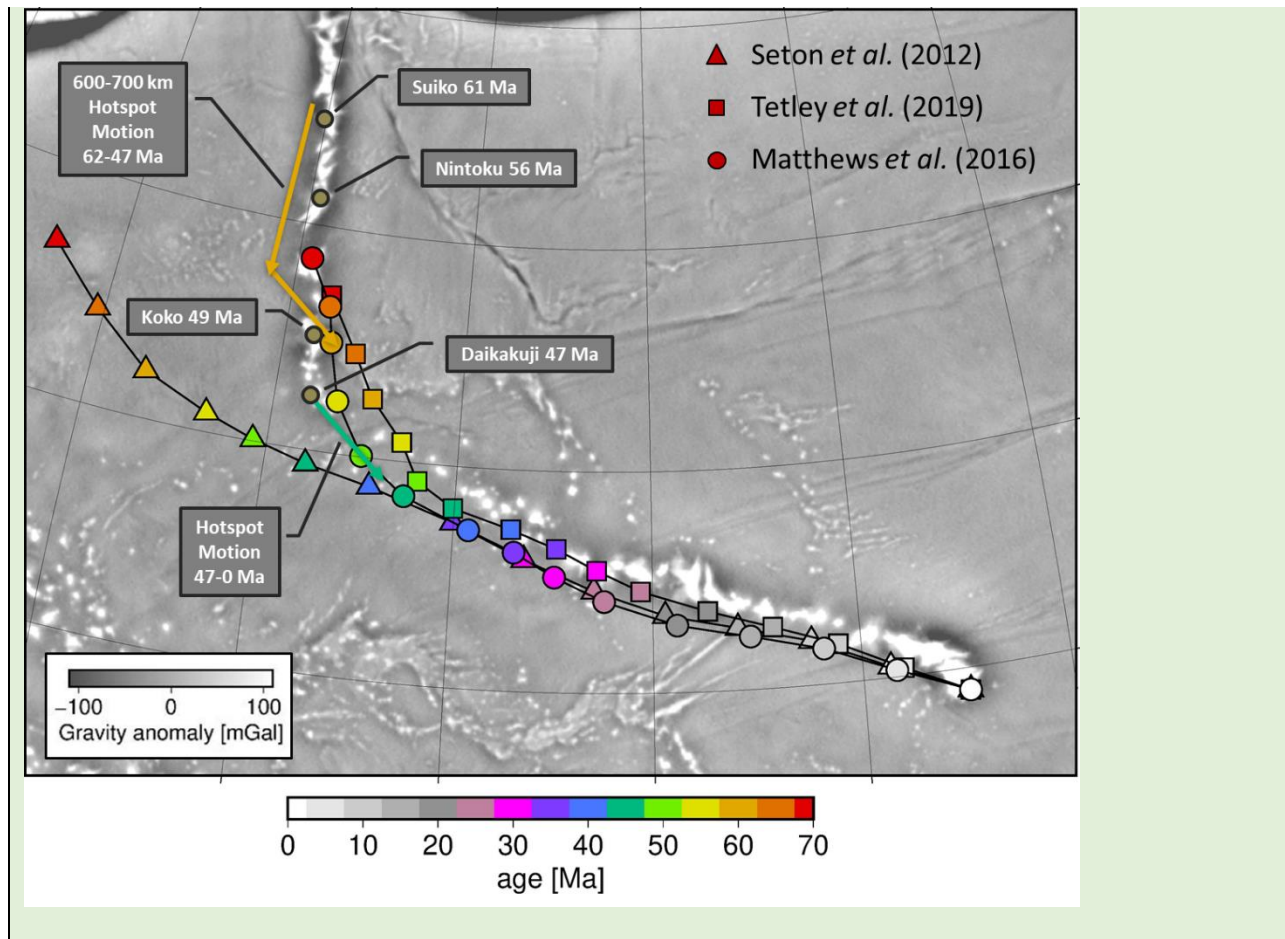
506 than plate tectonic movements (distinguishing plume motions). We also discuss how plumes provide  
507 insights into possible reorientations of the entire Earth relative to its spin axis (true polar wander) and  
508 how they are considered powerful initial agents in the global plate tectonic cycle (breaking up continents).

### 6.1 Distinguishing Plume Motions

509 The presumed stability of ‘thermal’ mantle plumes initially allowed scientists to use the shapes and age  
510 progressions of seamount trails to derive directions and speeds of past plate motions, and with those  
511 models in hand, to chart out the positions of tectonic plates back through geological time (e.g. Wilson  
512 1963; Morgan 1971; Minster and Jordan 1974; Duncan and Clague 1985; Müller *et al.* 1993; Koppers *et*  
513 *al.* 2001; Wessel and Kroenke 2008; Torsvik *et al.* 2014; Wessel and Conrad 2019). In these models,  
514 fixed mantle plumes were presumed to persist over more than one hundred million years. Expected would  
515 be that all seamount trails forming on a particular tectonic plate would record the same history of plate  
516 rotations around the same Euler poles and with the same angular velocities; and when plate motion  
517 changes occurred, the timing of the ‘bends’ (or turns) that would form in each seamount trail, would be  
518 contemporaneous ([Box 2](#)). In other words, it would be expected that the geometries between different  
519 seamount trails would be fixed and their chronologies identical.

520 Paleomagnetic inclination data from seamount trails indicate that plumes are in fact not stationary  
521 with respect to the spin axis (Tarduno *et al.* 2003, Koppers *et al.* 2012; Tarduno and Koppers 2019).  
522 Distance comparisons between coeval seamount trails show that plumes are moving away or closing in to  
523 each other (O'Connor *et al.* 2013; Konrad *et al.* 2018a) and the  $^{40}\text{Ar}/^{39}\text{Ar}$  dating of the Louisville and  
524 Rurutu hotspot tracks on the Pacific plate show that the most acute parts in their bends (not as pronounced  
525 or clearly visible as for Hawaii) appear to occur about 3 million earlier than the Hawaii-Emperor Bend  
526 around 47 million years ago (Sharp and Clague 2006; Koppers *et al.* 2011b; Finlayson *et al.* 2018;  
527 Konrad *et al.* 2018a) but their timing does coincide with the start of the Hawaii-Emperor bend around 50  
528 million years ago. For these Cretaceous and early Cenozoic times, the most recent analysis by Bono *et al.*  
529 (2019) of related paleomagnetic data and age dates concluded that the Hawaiian hotspot moved at  $48 \pm 8$   
530 mm/yr between 63 and 52 Ma, while other Pacific hotspots have moved much more slowly. Similarly,  
531 based on age progressions along tracks and changing distances between tracks, Konrad *et al.* (2018a)  
532 found a total relative motion of  $53 \pm 21$  mm/yr between Hawaii and Louisville and of  $57 \pm 27$  mm/yr  
533 between Hawaii and Rurutu, most likely due to a large individual Hawaiian hotspot motion from 60 to 48  
534 Ma. These observations are not unexpected in a convecting mantle, as computer simulations show that  
535 rising mantle plumes will be advected in Earth’s overall mantle circulation regime (Steinberger and  
536 O’Connell 1998; Steinberger 2000; Hassan *et al.* 2016; Arnould *et al.* 2019) causing the locations of  
537 hotspots on the Earth’s surface to wander over geological time.

538 **Box 2: Scenarios for the HEB Formation.** The prominent 120° bend in the Hawaii-Emperor seamount  
539 trail (HEB) was first interpreted as representative of a major change in Pacific plate motion (Duncan and  
540 Clague 1985) occurring around 47 million years ago (Sharp and Clague 2006). However, an absence of  
541 geological evidence for a change in Pacific plate motion at that time, and recognition that hotspots are  
542 mobile, led to the proposal that the HEB may rather represent Hawaiian hotspot motion, which came to a  
543 rather abrupt stop at the time of the bend (Norton 1995). This hypothesis was tested through the analyses  
544 of magnetic paleolatitudes in scientific ocean drilling cores recovered from Emperor seamounts, which  
545 support a significant southward hotspot motion between ~80 and 47 Ma (Tarduno and Cottrell 1997;  
546 Tarduno *et al.* 2003; Bono *et al.* 2019). Konrad *et al.* (2018a) compared the relative distances of Pacific  
547 hotspots using age progressions along three tracks (Hawaii, Louisville, Rurutu). The results show the  
548 Hawaiian hotspot moving southward, with most of the motion occurring between 62 and 47 million years  
549 ago, but with a maximum ~600-700 km of motion detected that is insufficient to explain the entire, more  
550 than 2,000 km length of the Emperor chain. There remains an active debate on the relative contribution of  
551 hotspot drift and plate motion changes to the shape of the 120° bend, with scenarios ranging from the  
552 HEB being entirely caused by a ~60° change in plate motion (Steinberger *et al.* 2004; Torsvik *et al.* 2017)  
553 to being mostly caused by hotspot drift (Bono *et al.* 2019; Hassan *et al.* 2016). The map shows modeled  
554 0-70 Ma tracks for a *fixed* Hawaii hotspot and three plate reconstructions that all use the Antarctic plate  
555 circuit. Matthews *et al.* (2016) and Tetley *et al.* (2019) use relative motions in Zealandia as additional  
556 constraints, whereas Seton *et al.* (2012) do not. A large body of work is suggesting a major plate  
557 reorganization at ~50 Ma centered around the Pacific Plate (e.g. Cosca *et al.* 1998; Meffre *et al.* 2012;  
558 Reagan *et al.* 2019), yet these plate motion models account for at most 35° of the expected 60° absolute  
559 plate motion change and cannot accurately predict the location and age of seamounts in the Hawaii-  
560 Emperor track prior to 30 million years ago. The mismatch between the predicted 47 Ma hotspot locations  
561 and the actual location of the bend (Daikakuji Seamount) is consistent with ~1 cm/yr SE hotspot motion  
562 (green arrow) from 47-0 Ma obtained by numerical models (Steinberger *et al.* 2004; Hassan *et al.* 2016).  
563 The mismatch between the predicted 61 Ma hotspot locations and Suiko Guyot can be amended by  
564 additional rapid southward hotspot motion (long orange arrow) that is consistent with age progressions  
565 along the hotspot tracks (Konrad *et al.* 2018a) and numerical modeling (Hassan *et al.* 2016). In this  
566 debate, however, it appears that a large portion of the length of the Emperor chain only can be explained  
567 by southward Hawaii hotspot drift.



568

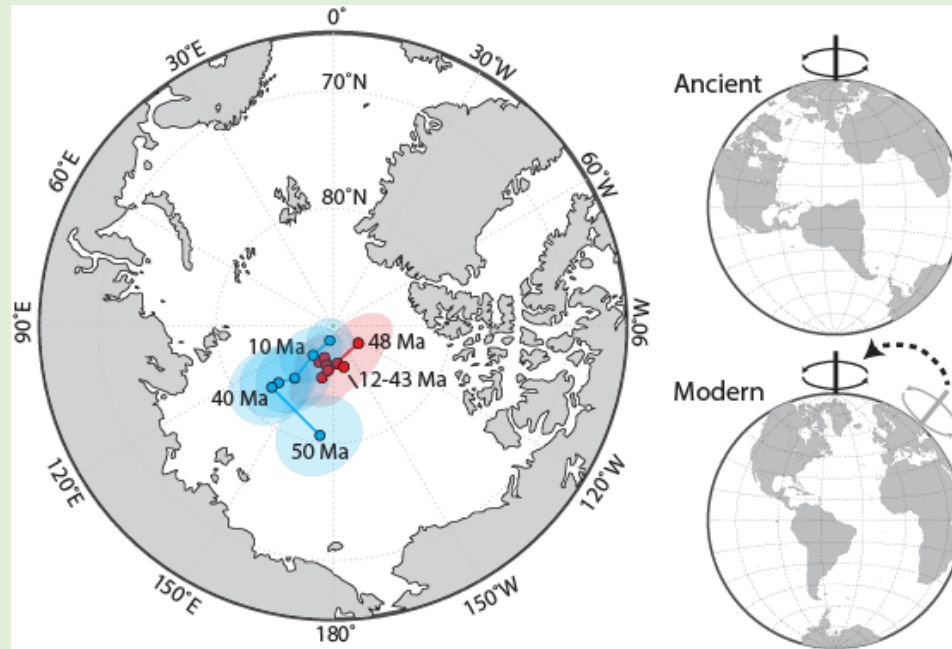
569 For the most recent 5 million years in Earth’s history, the rate of motion of major hotspots was  
 570 recently computed by Wang *et al.* (2018) using a maximum likelihood optimization that incorporated  
 571 present-day plate motion models and compared those to the azimuths and age progressions of hotspot  
 572 tracks (Morgan and Phipps Morgan 2007). They obtained highly variable hotspot motion rates between  
 573 2.5 mm/yr (Afar) and 49.4 mm/yr (Caroline) with Hawaii moving at 11.6 mm/yr. In this model, the  
 574 Pacific hotspots were found to move at speeds between 10 and 50 mm/yr, while Atlantic and Indian  
 575 Ocean hotspots would move more slowly, below 20 mm/yr. An alternative kinematics-based approach  
 576 was recently developed by Tetley *et al.* (2019) to determine the motions of major hotspots for the last 80  
 577 Ma by estimating misfits while fitting hotspot tracks and treating all hotspots as fixed. The resulting  
 578 hotspot trail misfits represent a robust estimate of hotspot motion, with rates generally below 40 mm/yr  
 579 for all major hotspots other than Hawaii (Tetley *et al.* 2019). However, using other modeling approaches,  
 580 the absolute plate motion reference frame for the present-day yields similar net rotations (i.e. wholesale  
 581 lithospheric spin of all tectonic plates with respect to a fixed lower mantle) for fixed or moving hotspot  
 582 assumptions (Becker *et al.* 2015). Likewise, other authors have used similar data, but only considering the  
 583 azimuth of hotspot trends, to conclude that there is no requirement for hotspots at the present day to move

584 at all, and that a fixed hotspot reference frame may fit the data better (Wang *et al.* 2019). These  
585 contrasting papers exemplify the extent of the ongoing controversy about hotspot motion.

586         Importantly, these scenarios now also can be compared to geodynamic models of hotspot motion.  
587 Steinberger and O'Connell (1998) pioneered an approach based on large-scale mantle flow models (see  
588 also Steinberger 2000; Doubrovine *et al.* 2012) in which mantle flow is computed based on density  
589 models inferred from 3D seismic tomography, assumed whole mantle viscosity profiles, and time-  
590 dependent plate motions as surface boundary conditions. The approach is completed by inserting initially  
591 vertical plume conduits that then are advected while buoyantly rising through the convecting mantle. In  
592 these geodynamic models the computed hotspot motions are typically slower than plate motions, mostly  
593 less than 1 cm/yr. This slow motion foremost is a consequence of plumes being anchored in, and rising  
594 from the lower mantle, which is only sluggishly convecting because of its high viscosity up to about  $10^{23}$   
595 Pa s. This geodynamic modeling approach is most reliable in the Cenozoic, but less so for earlier times, as  
596 backward-advection of mantle density anomalies becomes increasingly unreliable. The gap is now being  
597 filled with geodynamic forward models that can capture both the tilt of plume stems in the mantle as well  
598 as the motion of the plume generation zone (Hassan *et al.* 2015; 2016).

599 **Box 3: True Polar Wander.** Motion of the magnetic north pole as seen from a specific tectonic plate  
600 may be caused by plate motion and/or by re-orientation of the entire Earth relative to the poles. The  
601 former is termed apparent polar wander, the latter true polar wander. For approximately the last  
602 120 million years, plate motion can be determined from hotspot tracks, allowing a “true polar wander  
603 path” to be reconstructed by rotating a single plate back to its past locations in the hotspot reference  
604 frame, and transferring the corresponding paleomagnetic pole positions with it. The remainder trace of  
605 past pole positions then in theory equals the true polar wander path. In practice, true polar wander paths  
606 for different plates differ somewhat, due to non-dipolar components of the magnetic field and other  
607 uncertainties (e.g. Besse and Courtillot 2002; Torsvik *et al.* 2012), but they can be combined to devise a  
608 global true polar wander path. Two modeled paths with uncertainty ellipses representing 95% confidence  
609 by Doubrovine *et al.* 2012 (blue) and Woodworth and Gordon 2018 (red) are shown for the last 50  
610 million years relative to respectively global and Pacific hotspot reference frames, showing only minor  
611 true polar wander in this time frame. As true polar wander is expected from significant shifts in Earth's  
612 mass distribution (Gold, 1955) on geological timescales, it is likely to result from reconfigurations in  
613 large-scale mantle structures (Steinberger and O'Connell 1997). The two LLSVP superstructures are  
614 thought to be stable for hundreds of millions of years (Burke and Torsvik 2004; Torsvik *et al.* 2006;  
615 Burke *et al.* 2008; Dziewonski *et al.* 2010) and we can infer that the two corresponding antipodal geoid  
616 highs are also stable for the same amount of time. Since the spin axis remains aligned with the minimum

617 point of the spherical harmonic degree two geoid component—in between those two geoid highs—it is  
618 expected that true polar wander occurs in a “ring” around the Earth that runs in between the two LLSVPs  
619 and that it is mostly driven by the sinking of “heavy” lithospheric slabs subducting for a large part near  
620 that ring (Steinberger *et al.* 2017). The largest amount of true polar wander since 120 Ma that can be  
621 determined occurred at speeds in the order of 10 mm/yr, mostly between 100 and 110 million years ago,  
622 and closely following a direction going around that ring. True polar wander in any other period is less  
623 expected and less prominent.



624

## 6.2 Breaking Up Continents

625 Mantle plumes may play an active role in the breakup of continents and/or oceanic lithosphere, when they  
626 impinge those from beneath, providing a starting point for the Wilson Cycle in plate tectonics and a likely  
627 important initiation mechanism for far-field major plate reorganizations. Continental breakup occurs  
628 when enough extension occurs to split continental lithosphere and form a new ocean basin. Many of the  
629 continental flood basalt provinces in the Mesozoic and Cenozoic are closely related in time and space  
630 with continental breakup (Morgan 1971; Storey 1995; White and McKenzie 1989; Courtillot *et al.* 1999).  
631 When reconstructed back to their original plate tectonic configuration, flood basalt provinces are often  
632 found along continental margins, and dike swarms have more or less radial patterns and terminate at the  
633 margins of continental cratons (Burke and Dewey 1973; Fahrig and Schwarz 1973).

634 These observations led to the active continental rift hypothesis, where mantle plumes are thought  
635 to drive continental breakup. In this model, continental rifting is actively driven by mantle plume

636 processes, including arrival of a plume head at the base of the lithosphere, heating and erosion of the  
637 lithosphere, and heating, uplift and tensional failure of the mechanical lithosphere (Courillot *et al.* 1999).  
638 Alternatively, continental breakup may be explained by the passive rifting model, where continental  
639 rifting is driven by far-field tectonic forces and interaction with an existing plume is co-incident. In both  
640 scenarios, the combination of lithospheric extension and upwelling plume material causes abnormally  
641 large volumes of magma to erupt through passive decompression melting (White and McKenzie 1989). It  
642 also appears that most continental rifts without a plume failed, with only one third proceeding to break-up  
643 (Ziegler and Cloetingh 2004). The fact that continental rifting can extend from only a few million years  
644 up to around 100 million years before progressing to continental breakup, therefore, has called for a  
645 combination of passive and active plume head forces (Courillot *et al.* 1999).

646 For continental rifts that do proceed to breakup, plumes appear to play a triggering, but not an  
647 essential role. The role for plumes is particularly striking when the timing of continental rifting, flood  
648 basalt eruption, and continental break up are compared, with continental rifting often extending for tens of  
649 millions of years and—after this prolonged period—ending with the voluminous eruption of flood basalts  
650 that are coevally, or closely followed by, continental breakup (Buiter and Torsvik 2014). Brune *et al.*  
651 (2013) tested the role of plumes as a trigger for continental breakup by modelling lithosphere under far-  
652 field extension, investigating the role of plume-related lithospheric erosion, finding that plume erosion  
653 decreases lithospheric strength and controls the timing or even occurrence of continental breakup.

654 Finally, mantle plumes, along with changes in plate boundary forces (Whittaker *et al.* 2016,  
655 Gaina *et al.* 2009) and “wrench” tectonics (Nemcok *et al.* 2016) also are thought to drive the formation of  
656 microcontinents, small continental fragments that become separated from their parent continental margin  
657 and eventually surrounded by oceanic lithosphere. In these smaller scale manifestations of plate tectonics,  
658 mantle plumes have been implicated in the rifting and separating of microcontinents from relatively  
659 young continental margins, less than 25 million years old, through one or multiple mid-ocean ridge  
660 relocations that are centred around the mantle plume, resulting in ocean spreading asymmetries and ridge  
661 propagation towards the locus of the plume (Müller *et al.* 2001).

## 7. Mantle Plumes Impacting Earth’s Environment

662 Mantle plumes are the source of a phenomenal volume of volcanic products on the Earth’s surface (Coffin  
663 and Eldholm 1994). When mantle plumes cause hotspot volcanism, outputs are particularly high during  
664 plume head volcanism that causes a rapid outpouring of voluminous LIPs, in the oceans referred to as  
665 oceanic plateaus and on land as flood basalts. Emplacement of these LIPs is hypothesized to cause  
666 extreme global environmental perturbations and mass extinctions (Courillot *et al.* 1988; Duncan and Pyle  
667 1988; Renne *et al.* 2013). According to these hypotheses, flood basalt volcanism introduces large

668 quantities of volatiles such as sulfuric acid into the Earth's atmosphere (with SO<sub>2</sub> forming H<sub>2</sub>SO<sub>4</sub>) and  
669 carbon dioxide (CO<sub>2</sub>) release may be increased significantly, resulting in greenhouse scenarios (Kerr  
670 2005; Self 2006; Kerr 2014). In contrast, introduction of volcanic ash and aerosols in the Earth's  
671 atmosphere may cause shielding from solar radiation, leading to the cooling of global climate (Self 2006).  
672 Each of these processes may induce strong perturbations in the environment and trigger tipping points in  
673 Earth's climate state, with the increased extinction of species as one of the major outcomes. Geodynamic  
674 simulations also show that mantle plumes may have accumulated oxidized materials in the upper mantle  
675 and with that may have influenced the evolution of atmospheric oxygen (Gu *et al.* 2016).

676         However, it remains hard to undeniably link the causes and chronologies associated with global  
677 extinction events to mantle plume-induced eruptions. For example, emplacement of the Deccan Traps  
678 flood basalt seems to have started a few tens of thousands of years prior to the extinction at the K-Pg  
679 boundary around 66 million years ago, but it is now also apparent that more than 75% of Deccan Trap  
680 volcanism occurred following the Chicxulub meteorite impact (Renne *et al.* 2013; Schoene *et al.* 2019;  
681 Sprain *et al.* 2019). Similarly, emplacement of the Siberian Traps was extremely rapid, causing massive  
682 volcanism over a period of less than ten thousand years, but geochronological techniques lack resolution  
683 to definitely tie this flood basalt to the largest Earth extinction event at the Permo-Triassic boundary  
684 around 250 million years ago (Courtillet and Renne 2003; Reichow *et al.* 2009; Sobolev *et al.* 2011;  
685 Courtillet and Fluteau 2014). Even though plume-related volcanism resulting in voluminous flood basalts  
686 are likely to have direct impacts on global climate, from the Chicxulub impact event it appears that there  
687 are additional primary drivers that could tip over Earth's climate system and cause massive extinctions  
688 (Hull *et al.* 2020).

689         In the oceans, the impacts of large-scale mantle plume eruptions on the environment are different,  
690 yet allegedly they also cause widespread species extinction. These submarine eruptions may introduce  
691 toxic metals that poison marine life, or they may provide high levels of nutrients that cause planktonic  
692 blooms that then massively deprive the oceans of oxygen after these organisms die off and decompose  
693 (Sinton and Duncan 1997; Kerr 2005). These episodes are recognized as 'oceanic anoxic events' that are  
694 chronicled in marine sedimentary records through the deposition of black shales. The timing of ocean  
695 plateau formation relative to the formation of those globally dispersed black shales is still highly  
696 uncertain. Future scientific ocean drilling and modern-day geochronology is required to uniquely tie the  
697 formation of mantle plume-derived oceanic plateaus to these deadly global oceanic anoxic events.

## 8. Future Mantle Plume Research

698 Even though mantle plumes are sometimes considered independent of the key plate tectonic processes,  
699 such as plate spreading and subduction, mantle plumes in fact are an integral part of a dynamic Earth.

700 Mantle plumes are part of the overall ‘rock cycle’ in the Earth system, playing a key role in Earth’s  
701 overall convectational regime, and in the continuous recycling of Earth’s deep interior and surface  
702 materials. Many mantle plumes are originating from the deepest regions in Earth’s mantle, often in  
703 association with LLSVPs and ULVZs, and plumes potentially even take in materials from the Earth’s core  
704 itself. On the other end, at Earth’s surface, we see clear evidence of plume activity, in intra-plate  
705 volcanism, continental break-up, and long-term effects on Earth’s climate system. Yet, our knowledge of  
706 mantle plumes remains limited, largely because of the low-resolution view we have of their structures and  
707 behaviors through seismic mantle tomography studies, and because of the complexity of plume  
708 expressions in the volcanic structures (seamount trails, oceanic plateaus) on Earth’s surface. Below we  
709 compile a short list of future research themes where we can improve our understanding of mantle plumes  
710 themselves and their effects on the interconnected Earth system.

711 **Mantle Plume and LLSVP Imaging:** Reconciling current seismic images of “mantle plumes” with the  
712 geodynamic modeling and surface observations is THE challenge for the future. Large-scale deployments  
713 of OBS (ocean bottom seismometers) with wider apertures are required to create detailed views of the  
714 deep portions of mantle plumes. For example, we need to improve on the geometries and placement of  
715 OBS instruments and design them to capture specific seismic phases that can better resolve structures at  
716 the roots of mantle plumes and shed light on their potential generation in the LLSVP and ULVZ regions.

717 **Thermal versus Thermochemical Plumes:** What is the nature of the plumes that now start to get  
718 resolved by tomography in the lower mantle? Are they purely thermal or thermo-chemical and how do  
719 they relate to a potential basal dense layer? Do we need to explore more complex rheologies to explain  
720 their morphologies and temporal behaviors? We also need to understand how these plumes may interact  
721 with mantle flow and get deflected primarily in the 660-1,000 km depth range.

722 **Dynamic Topography:** The upwelling of mantle plumes may affect the dynamic topography of oceanic  
723 lithosphere (Conrad *et al.* 2004; Li and Zhong 2009; Zhang *et al.* 2010; Poore *et al.* 2011; Parnell-Turner  
724 *et al.* 2014; Steinberger *et al.* 2019a). Where the presence of strong or weak mantle plumes may cause  
725 large or small hotspots swells (King and Adam 2014) and regional modifications in mantle viscosity  
726 profiles, the ‘pulsating’ behavior of mantle plumes may cause significant variations in local sea level that  
727 may change ocean circulation patterns and deep-sea sedimentation accumulation rates (Parnell-Turner *et al.*  
728 *et al.* 2014). Gaps in understanding mantle viscosity profiles, in particular in the proximity of larger plume  
729 swells, are causing major uncertainties in modeling future sea level rise across the world (Müller 2010;  
730 Petersen *et al.* 2010; Rovere *et al.* 2015).

731 **Oceanic LIPs:** The formation and history of oceanic LIPs are still poorly understood compared to their  
732 extensively studied onshore counterparts. There is an intriguing association with spreading ridges and

733 triple junctions, which now appears to be archetypal for plumes in the ocean basins. The recent work on  
734 Shatsky Rise (Sager *et al.* 2013; 2019) reinforces the idea that some LIPs might not be caused by plume  
735 head eruptions, which raises interesting questions whether Shatsky is a headless plume interacting with  
736 the overriding oceanic lithosphere.

737 **Spherical Shell 3D Earth Modeling:** An exciting and growing field of mantle geodynamics involves the  
738 generation of three-dimensional spherical shell numerical models of the Earth that solve the governing  
739 equations for appropriate physical parameters. These models can evolve through geological time allowing  
740 us to study the interactions between tectonic processes, large-scale mantle flow, and plumes (e.g. Zhong  
741 *et al.* 2000; Zhong 2006; Tackley 2008; Arnould *et al.* 2019; 2020). The simulation output can then be  
742 used to interpret complex surface and seismic tomographic features. With advancements in  
743 supercomputing, it is expected that this style of 3D modeling will continue to advance and provide  
744 important insights into Earth's inner workings.

745 **Low-flux Hotspots:** Given the geological importance of linking chemical components observed in ocean  
746 island lava flows to underlying mantle features, future improvements in our understanding of the variable  
747 makeup of the mantle require joint geochemistry-geodynamics-geophysical research at various global  
748 hotspots. It is important to focus on other hotspot systems besides Hawaii, as that plume displays an  
749 anomalously high buoyancy flux relative to the global average for hotspots. Its high buoyancy and related  
750 melt flux have the potential to obscure geographic trends in plume-derived lava chemistry, which might  
751 be more easily discernable at low-flux hotspots (Chauvel *et al.* 2012).

752 **Enriched and Primordial Mantle Domains:** Over the last half a century geochemical studies caused a  
753 paradigm shift in our understanding of the makeup of the mantle—which represents 84% of Earth's  
754 volume—from a homogenous material body to a complex mix of mantle domains each characterized by a  
755 different heritage and geological history. We still have limited ideas on the time and length scales of these  
756 domains, where they reside, and what is their long-term stability.

757 **Coordinating Geochemical Efforts:** In terms of geochemistry, a better effort must be made to  
758 coordinate geochemical and isotopic and geochronological analyses on the same samples, in particular for  
759 multiple novel short-lived isotopic systems. For example, we have no idea how  $^{129}\text{Xe}$  anomalies (which  
760 track the degassing history of the planet) relate to  $^{182}\text{W}$  anomalies (which track core formation) because  
761 exactly *one* rock has been characterized for both isotopic systems, but this sample was not characterized  
762 for  $^{142}\text{Nd}$  (which tracks silicate Earth differentiation). Understanding the earliest history of the planet will  
763 require a multi-proxy effort with coordination across laboratories.

764 **Cyclicities in Global Intra-Plate Volcanism and Plume Life Spans:** Over the last 200 million years a  
765 waxing and waning of global intra-plate volcanism (Larson 1991b) and ocean crust formation (Müller *et*

766 *al.* 2008) is observed, but drivers and potential links between these cyclicities are unknown. Future research  
767 needs to provide process-based understanding and whether plume formation through time can be linked to  
768 coupled plate tectonic and mantle evolution, and to cycles of plate aggregation, dispersal, and subduction.  
769 Related to this is figuring out why plumes have such a long range of life spans, anything from ~30 to 150  
770 million years and longer, and how their roles changed as a function of a decreasing internal heat production  
771 over Earth's history.

772 **Transition Zone Plumes:** The modes of rising mantle plumes and from which depths they originate is  
773 still under debate. For example, we don't know if "transition zone plumes" exist, and if so, if they form  
774 by ponding of superplumes on 660 km mantle discontinuity (e.g. Tan *et al.* 2002), if they are deflected  
775 deep plumes, or if they are the natural consequence of asthenospheric convection related to the subduction  
776 process and slab induced hydration of the transition zone (e.g. Faccenna *et al.* 2010).

777 **Global Plume Heat Flux:** Another enigma relates to figuring out whether the overall global plume flux  
778 is consistent with the balance between the heat flux across the core-mantle boundary, internal heating, and  
779 the thermal evolution of Earth.

780 **Solid Earth, Climate and Biosphere Interactions:** Mantle plume activity results in extensive volcanism  
781 on Earth's surface with impacts for its environment, and all forms of life on this planet. A key challenge  
782 is to capture the complete chronologies that record the mantle plume events that produce flood basalts and  
783 oceanic plateaus, and to tie those to other geological records—such as sedimentary records on land and in  
784 subseafloor scientific ocean drilling cores—that contain information about Earth's environment, species  
785 extinction, ocean chemistry, ocean acidification, oxygenation, and more. We need those records to help  
786 figure out how relevant plumes are in solid Earth, climate and biosphere interactions, including their  
787 impacts on long-term climate change, mass extinctions, and biosystem resiliency.

## 9. Acknowledgements

788 The authors are supported by the National Science Foundation (NSF) grants OCE-1912932 (AAPK, KK),  
789 EAR-1900652 (MGJ) and EAR-1758198 (BR); National Aeronautics and Space Administration (NASA)  
790 grant OSP 201601412-001 (TWB); Centre of Excellence project 223272 through the Research Council of  
791 Norway (BS), and the Australian Research Council (ARC) grant IH130200012 (RDM).

## 10. References

792 Abouchami, W., A.W. Hofmann, S.J.G. Galer, F.A. Frey, J. Eisele and M. Felgenson (2005). Lead isotopes  
793 reveal bilateral asymmetry and vertical continuity in the Hawaiian mantle plume. *Nature* 434(7035):  
794 851-856.

795 Albers, M., and U.R. Christensen (1996), The excess temperature of plumes rising from the core-mantle  
796 boundary, *Geophysical Research Letters* 23: 3567-3570, DOI: 10.1029/96GL03311.

797 Allègre, C.J. (1982). Chemical geodynamics. *Tectonophysics* 81: 109-132.

798 Allègre, C.J., Thomas Staudacher, Philippe Sarda & Mark Kurz (1983). Constraints on evolution of Earth's  
799 mantle from rare gas systematics. *Nature* 30, 762-766.

800 Allen, R.M., G. Nolet, W.J. Morgan, K. Vogfjord, M. Nettles, G. Ekstrom, B.H. Bergsson, P. Erlendsson,  
801 G.R. Foulger, S. Jakobsdottir, B.R. Julian, M. Pritchard, S. Ragnarsson and R. Stefansson (2002).  
802 Plume-driven plumbing and crustal formation in Iceland. *Journal of Geophysical Research-Solid Earth*  
803 107(B8): ESE 4-1-ESE 4-19. DOI: Artn 2163 10.1029/2001jb000584

804 Anderson, D. (1982). Hotspots, polar wander, Mesozoic convection and the geoid, *Nature* 297: 391-393.  
805 DOI: 10.1038/297391a0

806 Anderson, D.L. (2013). The persistent mantle plume myth. *Australian Journal of Earth Sciences* 60: 657-  
807 673. DOI: 10.1080/08120099.2013.835283

808 Anderson, D.L. and J.H. Natland (2014). Mantle updrafts and mechanisms of oceanic volcanism.  
809 *Proceedings of the National Academy of Sciences* DOI: 10.1073/pnas.1410229111

810 Arnould, M., J. Ganne, N. Coltice and X. Feng (2019). Northward drift of the Azores plume in the Earth's  
811 mantle, *Nature Communications* 10, 3235, DOI: 10.1038/s41467-019-11127-7

812 Arnould, M., N. Coltice, N. Flament and C. Mallard (2020). Plate tectonics and mantle controls on plume  
813 dynamics. *Earth and Planetary Science Letters* 547: 116439. DOI: 10.1016/j.epsl.2020.116439.

814 Austermann, J., B. T. Kaye, J. Mitrovica, P. Huybers (2014) A statistical analysis of the correlation between  
815 large igneous provinces and lower mantle seismic structure, *Geophys. J. Int.*, 197, 1-9.

816 Ballmer, M. D., Schumacher, L., Lekic, V., Thomas, C., and Ito, G. (2016), Compositional layering within  
817 the large low shear-wave velocity provinces in the lower mantle, *Geochem. Geophys. Geosyst.*, 17,  
818 5056– 5077, doi:10.1002/2016GC006605.

819 Ballmer, M., Ito, G., van Hunen, J., and Tackley, P.J. (2011). Spatial and temporal variability in Hawaiian  
820 hotspot volcanism induced by small-scale convection. *Nature Geoscience* 4, 457-460. DOI:  
821 10.1038/ngeo1187

822 Ballmer, M.D., C. Houser, J.W. Hernlund, R.M. Wentzcovitch and K. Hirose (2017). Persistence of strong  
823 silica-enriched domains in the Earth's lower mantle. *Nature Geoscience* 10(3): 236-241. DOI:  
824 10.1038/Ngeo2898

825 Ballmer, M.D., Ito, G., Wolfe, C.J., Solomon, S.C. (2013). Double layering of a thermochemical plume in  
826 the upper mantle beneath Hawaii. *Earth Planet. Sci. Lett.*, 376 155-164.  
827 doi:10.1016/j.epsl.2013.06.022

828 Becker, T. W., Schaeffer, A. J., Lebedev, S., & Conrad, C. P. (2015). Toward a generalized plate motion  
829 reference frame. *Geophysical Research Letters*, 42(9), 3188-3196.

830 Becker, T.W. and L. Boschi (2002). A comparison of tomographic and geodynamic mantle models.  
831 *Geochemistry, Geophysics, Geosystems* 3(1) DOI: 10.1029/2001gc000168

832 Becker, T.W., J.B. Kellogg and R.J. O'Connell (1999). Thermal constraints on the survival of primitive  
833 blobs in the lower mantle. *Earth and Planetary Science Letters* 171(3): 351-365. DOI: Doi  
834 10.1016/S0012-821x(99)00160-0

835 Besse, J., & Courtillot, V. (2002). Apparent and true polar wander and the geometry of the geomagnetic  
836 field over the last 200 Myr. *Journal of Geophysical Research: Solid Earth*, 107(B11), EPM-6.

837 Bijwaard, H. and W. Spakman (1999). Tomographic evidence for a narrow whole mantle plume below  
838 Iceland. *Earth and Planetary Science Letters* 166(3-4): 121-126. DOI: 10.1016/S0012-821x(99)00004-  
839 7

840 Bono, R. K., Tarduno, J. A., & Bunge, H. P. (2019). Hotspot motion caused the Hawaiian-Emperor Bend  
841 and LLSVPs are not fixed. *Nature communications*, 10(1), 1-9.

842 Boschi, L. and T.W. Becker (2011). Vertical coherence in mantle heterogeneity from global seismic data.  
843 *Geophysical Research Letters* 38(20) DOI: Artn L20306 10.1029/2011gl049281

844 Boschi, L., T.W. Becker and B. Steinberger (2007). Mantle plumes: Dynamic models and seismic images.  
845 *Geochemistry Geophysics Geosystems* 8(10) DOI: Artn Q10006. DOI:10.1029/2007gc001733

846 Boschi, L., T.W. Becker and B. Steinberger (2008). On the statistical significance of correlations between  
847 synthetic mantle plumes and tomographic models, *Physics of the Earth and Planetary Interiors*, 167,  
848 230-238, DOI: 10.1016/j.pepi.2008.03.009

849 Bossmann, A.B. and P.E. van Keken (2013). Dynamics of plumes in a compressible mantle with phase  
850 changes: Implications for phase boundary topography. *Physics of the Earth and Planetary Interiors*  
851 224: 21-31. DOI: 10.1016/j.pepi.2013.09.002

852 Bouvier, A. and M. Boyet (2016). Primitive Solar System materials and Earth share a common initial  
853 (142)Nd abundance. *Nature* 537(7620): 399-402. DOI: 10.1038/nature19351.

854 Boyet, M. and R.W. Carlson (2005). 142Nd evidence for early (>4.53 Ga) global differentiation of the  
855 silicate Earth. *Science* 309(5734): 576-581. DOI: 10.1126/science.1113634.

856 Brune, S., Popov, A.A. and Sobolev, S.V. (2013). Quantifying the thermo-mechanical impact of plume  
857 arrival on continental break-up. *Tectonophysics*, 604, pp.51-59.

858 Buitter, S.J. and Torsvik, T.H. (2014). A review of Wilson Cycle plate margins: A role for mantle plumes in  
859 continental break-up along sutures?. *Gondwana Research*, 26(2), pp.627-653.

860 Bull, A.L., M. Domeier and T.H. Torsvik (2014). The effect of plate motion history on the longevity of  
861 deep mantle heterogeneities. *Earth and Planetary Science Letters* 401: 172-182. DOI:  
862 10.1016/j.epsl.2014.06.008.

863 Burke, K. and Dewey, J.F. (1973). Plume-generated triple junctions: key indicators in applying plate  
864 tectonics to old rocks. *The Journal of Geology*, 81(4), pp.406-433.

865 Burke, K. and T.H. Torsvik (2004). Derivation of Large Igneous Provinces of the past 200 million years  
866 from long-term heterogeneities in the deep mantle. *Earth and Planetary Science Letters* 227(3-4):  
867 531-538. DOI: 10.1016/j.epsl.2004.09.015

868 Burke, K., B. Steinberger, T.H. Torsvik and M.A. Smethurst (2008). Plume Generation Zones at the  
869 margins of Large Low Shear Velocity Provinces on the core–mantle boundary. *Earth and Planetary  
870 Science Letters* 265(1-2): 49-60. DOI: 10.1016/j.epsl.2007.09.042

871 Burkhardt, C., L.E. Borg, G.A. Brennecka, Q.R. Shollenberger, N. Dauphas and T. Kleine (2016). A  
872 nucleosynthetic origin for the Earth's anomalous (142)Nd composition. *Nature* 537(7620): 394-398.  
873 DOI: 10.1038/nature18956.

874 Butterworth, N.P., A.S. Talsrna, R.D. Muller, M. Seton, H.P. Bunge, B.S.A. Schuberth, G.E. Shephard and  
875 C. Heine (2014). Geological, tomographic, kinematic and geodynamic constraints on the dynamics of  
876 sinking slabs. *Journal of Geodynamics* 73: 1-13. DOI: 10.1016/j.jog.2013.10.006.

877 Cabral, R.A., M.G. Jackson, E.F. Rose-Koga, K.T. Koga, M.J. Whitehouse, M.A. Antonelli, J. Farquhar, J.M.  
878 Day and E.H. Hauri (2013). Anomalous sulphur isotopes in plume lavas reveal deep mantle storage  
879 of Archaean crust. *Nature* 496(7446): 490-493. DOI: 10.1038/nature12020

880 Campbell, I.H. (2007). Testing the plume theory. *Chemical Geology* 241(3-4): 153-176. DOI:  
881 10.1016/j.chemgeo.2007.01.024

882 Carlson, R.W. and M. Boyet (2009). Short-lived radionuclides as monitors of early crust-mantle  
883 differentiation on the terrestrial planets. *Earth and Planetary Science Letters* 279(3-4): 147-156. DOI:  
884 10.1016/j.epsl.2009.01.017

885 Caro, G. and B. Bourdon (2010). Non-chondritic Sm/Nd ratio in the terrestrial planets: Consequences for  
886 the geochemical evolution of the mantle crust system. *Geochimica et Cosmochimica Acta* 74(11):  
887 3333-3349. DOI: DOI 10.1016/j.gca.2010.02.025.

888 Castillo, P. (1988). The DUPAL anomaly as a trace of the upwelling lower mantle. *Nature*, 336(6200),  
889 667–670. <https://doi.org/10.1038/336667a0>

890 Castillo, P.R. (2015). The recycling of marine carbonates and sources of HIMU and FOZO ocean island  
891 basalts. *Lithos* 216: 254-263. DOI: 10.1016/j.lithos.2014.12.005.

892 Chauvel, C., R.C. Maury, S. Blais, E. Lewin, H. Guillou, G. Guille, P. Rossi and M.A. Gutscher (2012). The  
893 size of plume heterogeneities constrained by Marquesas isotopic stripes. *Geochemistry Geophysics*  
894 *Geosystems* 13(7) DOI: Artn Q07005 10.1029/2012gc004123.

895 Clouard, V. and A. Bonneville (2001). How many Pacific hotspots are fed by deep-mantle plumes?  
896 *Geology* 29(8): 695-698.

897 Coffin, M.F. and O. Eldholm (1994). Large Igneous Provinces - Crustal Structure, Dimensions, and  
898 External Consequences. *Reviews of Geophysics* 32(1): 1-36. DOI: 10.1029/93rg02508

899 Collerson, K.D., Q. Williams, A.E. Ewart and D.T. Murphy (2010). Origin of HIMU and EM-1 domains  
900 sampled by ocean island basalts, kimberlites and carbonatites: The role of CO<sub>2</sub>-fluxed lower mantle  
901 melting in thermochemical upwellings. *Physics of the Earth and Planetary Interiors* 181(3-4): 112-  
902 131. DOI: 10.1016/j.pepi.2010.05.008

903 Conrad, C. P., Lithgow-Bertelloni, C., & Loudon, K. E. (2004). Iceland, the Farallon slab, and dynamic  
904 topography of the North Atlantic. *Geology*, 32(3), 177-180.

905 Cosca, M., Arculus, R., Pearce, J., and Mitchell, J. (1998). 40Ar/39Ar and K–Ar geochronological age  
906 constraints for the inception and early evolution of the Izu–Bonin–Mariana arc system. *Island Arc*,  
907 7(3), 579-595.

908 Cottaar, S. and B. Romanowicz (2012). An unusually large ULVZ at the base of the mantle near Hawaii.  
909 *Earth and Planetary Science Letters* 355: 213-222. DOI: 10.1016/j.epsl.2012.09.005

910 Courtillot, V. and F. Fluteau (2014). A review of the embedded time scales of flood basalt volcanism with  
911 special emphasis on dramatically short magmatic pulses. 505: 301-317. DOI: 10.1130/2014.2505(15)

912 Courtillot, V., A. Davaille, J. Besse and J. Stock (2003). Three distinct types of hotspots in the Earth's  
913 mantle. *Earth and Planetary Science Letters* 205(3-4): 295-308. DOI: 10.1016/S0012-821x(02)01048-  
914 8

- 915 Courtillot, V., C. Jaupart, I. Manighetti, P. Tapponnier and J. Besse (1999). On causal links between flood  
916 basalts and continental breakup. *Earth Planet. Sci. Lett.* 166(3-4): 177-195. DOI: Doi 10.1016/S0012-  
917 821x(98)00282-9.
- 918 Courtillot, V., G. Féraud, H. Maluski, D. Vandamme, M.G. Moreau and J. Besse (1988). Deccan flood  
919 basalts and the Cretaceous/Tertiary boundary. *Nature* 333(6176): 843-846. DOI: 10.1038/333843a0
- 920 Courtillot, V.E. and P.R. Renne (2003). On the ages of flood basalt events. *Comptes Rendus Geoscience*  
921 335(1): 113-140.
- 922 Dana, J. D. (1849). *Geology, United States Exploring Expedition, during the years 1838–1839, 1840, 1841,*  
923 *1842 Vol 10 (C. Sherman, Philadelphia, 1849).*
- 924 Dannberg, J. and R. Gassmöller (2018). Chemical trends in ocean islands explained by plume–slab  
925 interaction. *Proceedings of the National Academy of Sciences* 115(17): 4351-4356. DOI:  
926 10.1073/pnas.1714125115
- 927 Dannberg, J. and S.V. Sobolev (2015). Low-buoyancy thermochemical plumes resolve controversy of  
928 classical mantle plume concept. *Nat Commun* 6(1): 6960. DOI: 10.1038/ncomms7960.
- 929 Davaille A. and B. Romanowicz (2020) Deflating the LLSVPs: Bundles of mantle thermochemical plumes  
930 rather than thick stagnant "piles", in revision, *Tectonics*.
- 931 Davaille, A. (1999). Simultaneous generation of hotspots and superswells by convection in a  
932 heterogeneous planetary mantle. *Nature*, 402(6763), 756-760.
- 933 Davaille, A., F. Girard and M. Le Bars (2002). How to anchor hotspots in a convecting mantle? *Earth and*  
934 *Planetary Science Letters* 203(2): 621-634. DOI: 10.1016/s0012-821x(02)00897-x
- 935 Davaille, A., P. Carrez and P. Cordier (2018). Fat Plumes May Reflect the Complex Rheology of the Lower  
936 Mantle. *Geophysical Research Letters* 45(3): 1349-1354. DOI: 10.1002/2017gl076575
- 937 Davies, D. R., S. Goes and M. Sambridge (2015a) On the relationship between volcanic hotspot locations,  
938 the reconstructed eruption sites of large igneous provinces and deep mantle seismic structure, *EPSL*,  
939 411, 121-130.
- 940 Davies, D.R., N. Rawlinson, G. Iaffaldano and I.H. Campbell (2015b). Lithospheric controls on magma  
941 composition along Earth's longest continental hotspot track. *Nature* 525(7570): 511-514. DOI:  
942 10.1038/nature14903
- 943 Davies, D.R., S. Goes, J.H. Davies, B.S.A. Schuberth, H.P. Bunge and J. Ritsema (2012). Reconciling  
944 dynamic and seismic models of Earth's lower mantle: The dominant role of thermal heterogeneity.  
945 *Earth and Planetary Science Letters* 353: 253-269. DOI: 10.1016/j.epsl.2012.08.016
- 946 Davies, G.F. (1988). Ocean Bathymetry and Mantle Convection .1. Large-Scale Flow and Hotspots.  
947 *Journal of Geophysical Research-Solid Earth and Planets* 93(B9): 10467-10480. DOI:  
948 10.1029/JB093iB09p10467
- 949 Davies, J.H. (2005). Steady plumes produced by downwellings in Earth-like vigor spherical whole mantle  
950 convection models. *Geochemistry Geophysics Geosystems* 6(12) DOI: 10.1029/2005gc001042
- 951 Debaille V, Armytage R, Wainwright A, Pourkhorsandi H & Hublet G (2019). Neodymium Nucleosynthetic  
952 Anomalies in Chondrites, the End of the Story? *Goldschmidt Abstracts*, 2019 751

953 Delavault, H., C. Chauvel, E. Thomassot, C.W. Devey and B. Dazas (2016). Sulfur and lead isotopic  
954 evidence of relic Archean sediments in the Pitcairn mantle plume. *Proc Natl Acad Sci U S A* 113(46):  
955 12952-12956. DOI: 10.1073/pnas.1523805113

956 DePaolo, D.J., J.G. Bryce, A. Dodson, D.L. Shuster and B.M. Kennedy (2001). Isotopic evolution of Mauna  
957 Loa and the chemical structure of the Hawaiian plume. *Geochemistry Geophysics Geosystems* 2(7):  
958 doi:10.1029/2000GC000139.

959 Deschamps, F., E. Kaminski and P.J. Tackley (2011). A deep mantle origin for the primitive signature of  
960 ocean island basalt. *Nature Geoscience* 4(12): 879-882. DOI: 10.1038/Ngeo1295

961 Domeier, M., P.V. Doubrovine, T.H. Torsvik, W. Spakman and A.L. Bull (2016). Global correlation of lower  
962 mantle structure and past subduction. *Geophysical Research Letters*, 43, 4945-4953, DOI:  
963 10.1002/2016GL068827.

964 Doubrovine, P. V., B. Steinberger and T. H. Torsvik (2016) A failure to reject: Testing the correlation  
965 between large igneous provinces and deep mantle structures with EDF statistics, *Geochem.*  
966 *Geophys. Geosyst.*,17, 1130-1163, doi:10.1002/2015GC006044.

967 Doubrovine, P.V., B. Steinberger and T.H. Torsvik (2012). Absolute plate motions in a reference frame  
968 defined by moving hotspots in the Pacific, Atlantic and Indian oceans. *Journal of Geophysical*  
969 *Research*, 117, B09101, DOI: 10.1029/2011JB009072

970 Doucet, L.S., Z.-X. Li, R.E. Ernst, U. Kirscher, H.G. El Dien and R.N. Mitchell (2020). Coupled  
971 supercontinent–mantle plume events evidenced by oceanic plume record. *Geology* 48(2): 159-163.

972 Duncan, R.A. and D.A. Clague (1985). Pacific plate motion recorded by linear volcanic chains. The ocean  
973 basins and margins. A.E.A. Nairn, F.L. Stehli and S. Uyeda. New York, Plenum Press. 7A: The Pacific  
974 ocean: 89-121.

975 Dziewonski, A. M., B.H. Hager and R. J O'Connell (1977) Large-Scale Heterogeneities in the Lower  
976 Mantle, *J. Geophys. Res.*, 82, 239-255.

977 Dziewonski, A.M. and J.H. Woodhouse (1987). Global images of the Earth's interior, *Science*, 236: 37-48,  
978 DOI: 10.1126/science.236.4797.37

979 Dziewonski, A.M., V. Lekic and B.A. Romanowicz (2010). Mantle Anchor Structure: An argument for  
980 bottom up tectonics. *Earth and Planetary Science Letters* 299(1-2): 69-79. DOI:  
981 10.1016/j.epsl.2010.08.013

982 Eiler, J.M., K.A. Farley, J.W. Valley, A.W. Hofmann and E.M. Stolper (1996). Oxygen isotope constraints  
983 on the sources of Hawaiian volcanism. *Earth and Planetary Science Letters* 144(3-4): 453-468.

984 Eisele, Jürgen, Mukul Sharma, Stephen J.G. Galer, Janne Blichert-Toft, Colin W. Devey, Albrecht W.  
985 Hofmann (2002). The role of sediment recycling in EM-1 inferred from Os, Pb, Hf, Nd, Sr isotope and  
986 trace element systematics of the Pitcairn hotspot. *Earth and Planetary Science Letters* 196 (2002)  
987 197-212

988 Ernst, R.E. and K.L. Buchan (2003). Recognizing mantle plumes in the geological record. *Annual Review*  
989 *of Earth and Planetary Sciences*, 31: 469-523, DOI: 10.1146/annurev.earth.31.100901.145500

990 Faccenna, C., T.W. Becker, S. Lallemand, Y. Lagabriele, F. Funiciello and C. Piromallo (2010). Subduction-  
991 triggered magmatic pulses: A new class of plumes? *Earth and Planetary Science Letters* 299(1-2): 54-  
992 68. DOI: 10.1016/j.epsl.2010.08.012

- 993 Fahrig, W.F. and Schwarz, E.J. (1973). Additional paleomagnetic data on the Baffin diabase dikes and a  
994 revised Franklin pole. *Canadian Journal of Earth Sciences*, 10(4), pp.576-581.
- 995 Farnetani, C.G. (1997). Excess temperature of mantle plumes: The role of chemical stratification across  
996 D", *Geophysical Research Letters*, 24: 1583-1586, DOI: 10.1029/97GL01548
- 997 Farnetani, C.G. and A.W. Hofmann (2010). Dynamics and internal structure of the Hawaiian plume. *Earth  
998 and Planetary Science Letters* 295(1-2): 231-240. DOI: 10.1016/j.epsl.2010.04.005
- 999 Farnetani, C.G. and H. Samuel (2005). Beyond the thermal plume paradigm, *Geophysical Research  
1000 Letters*, 32, L07311. DOI: 10.1029/2005GL022360
- 1001 Farnetani, C.G., A.W. Hofmann and C. Class (2012). How double volcanic chains sample geochemical  
1002 anomalies from the lowermost mantle. *Earth and Planetary Science Letters* 359: 240-247. DOI:  
1003 10.1016/j.epsl.2012.09.057
- 1004 Farquhar, J., B.A. Wing, K.D. McKeegan, J.W. Harris, P. Cartigny and M.H. Thiemens (2002). Mass-  
1005 independent sulfur of inclusions in diamond and sulfur recycling on early Earth. *Science* 298(5602):  
1006 2369-2372. DOI: 10.1126/science.1078617.
- 1007 Finlayson, V.A., J.G. Konter, K. Konrad, A.A.P. Koppers, M.G. Jackson and T.O. Rooney (2018). Sr–Pb–Nd–  
1008 Hf isotopes and <sup>40</sup>Ar/<sup>39</sup>Ar ages reveal a Hawaii–Emperor-style bend in the Rurutu hotspot. *Earth  
1009 and Planetary Science Letters* 500: 168-179. DOI: 10.1016/j.epsl.2018.08.020
- 1010 Foulger, G.R. and J.H. Natland (2003). Is "hotspot" volcanism a consequence of plate tectonics? *Science*  
1011 300(5621): 921-922. DOI: 10.1126/science.1083376
- 1012 French, S.W. and B.A. Romanowicz (2014). Whole-mantle radially anisotropic shear velocity structure  
1013 from spectral-element waveform tomography. *Geophysical Journal International* 199(3): 1303-1327.  
1014 DOI: 10.1093/gji/ggu334
- 1015 French, S.W. and B. Romanowicz (2015). Broad plumes rooted at the base of the Earth's mantle beneath  
1016 major hotspots. *Nature* 525(7567): 95-99. DOI: 10.1038/nature14876
- 1017 Frey, F. A., & Rhodes, J. M. (1993). Intershield geochemical differences among Hawaiian volcanoes:  
1018 Implications for source compositions, melting process and magma ascent paths. *Philosophical  
1019 Transactions of the Royal Society of London. Series A: Physical and Engineering Sciences*, 342(1663),  
1020 121-136.
- 1021 Frost, D.A. and S. Rost (2014). The P-wave boundary of the Large-Low Shear Velocity Province beneath  
1022 the Pacific. *Earth and Planetary Science Letters* 403: 380-392. DOI: 10.1016/j.epsl.2014.06.046.
- 1023 Fukao, Y. and M. Obayashi (2013). Subducted slabs stagnant above, penetrating through, and trapped  
1024 below the 660 km discontinuity. *Journal of Geophysical Research-Solid Earth* 118(11): 5920-5938.  
1025 DOI: 10.1002/2013jb010466
- 1026 Gaina, C., L. Gernigon and P. Ball (2009). Palaeocene-Recent plate boundaries in the NE Atlantic and the  
1027 formation of the Jan Mayen microcontinent. *Journal of the Geological Society* 166(4): 601-616. DOI:  
1028 10.1144/0016-76492008-112
- 1029 Garapić, G., M. Jackson, E. Hauri, S. Hart, K. Farley, J. Blusztajn and J. Woodhead (2015). A radiogenic  
1030 isotopic (He-Sr-Nd-Pb-Os) study of lavas from the Pitcairn hotspot: Implications for the origin of EM-  
1031 1 (enriched mantle 1). *Lithos* 228: 1-11.
- 1032 Garnero, E.J., A.K. McNamara and S.H. Shim (2016). Continent-sized anomalous zones with low seismic  
1033 velocity at the base of Earth's mantle. *Nature Geoscience* 9(7): 481-489. DOI: 10.1038/Ngeo2733

- 1034 Gleeson, M.L.M., S.A. Gibson and H.M. Williams (2020). Novel insights from Fe-isotopes into the  
1035 lithological heterogeneity of Ocean Island Basalts and plume-influenced MORBs. *Earth and Planetary*  
1036 *Science Letters* 535: 116114. DOI: ARTN 116114 10.1016/j.epsl.2020.116114
- 1037 Gold, T. (1955). Instability of the Earth's axis of rotation. *Nature* 175(4456): 526-529.
- 1038 Grand, S.P., R.D. van der Hilst and S. Widiyantoro (1997). High resolution global tomography: a snapshot  
1039 of convection in the Earth. *Geological Society of America Today* 7(4).
- 1040 Gu, T.T., M.M. Li, C. McCammon and K.K.M. Lee (2016). Redox-induced lower mantle density contrast  
1041 and effect on mantle structure and primitive oxygen. *Nature Geoscience* 9(9): 723-+. DOI:  
1042 10.1038/Ngeo2772
- 1043 Gülcher, A.J.P., D.J. Gebhardt, M.D. Ballmer and P.J. Tackley (2020). Variable dynamic styles of  
1044 primordial heterogeneity preservation in the Earth's lower mantle. *Earth and Planetary Science*  
1045 *Letters* 536: 116160. DOI: 10.1016/j.epsl.2020.116160
- 1046 Hager, B.H., R.W. Clayton, M.A. Richards, R.P. Comer and A.M. Dziewonski (1985). Lower Mantle  
1047 Heterogeneity, Dynamic Topography and the Geoid. *Nature* 313(6003): 541-546.  
1048 DOI:10.1038/313541a0.
- 1049 Halliday, A.N. (2004). Mixing, volatile loss and compositional change during impact-driven accretion of  
1050 the Earth. *Nature* 427(6974): 505-509. DOI: 10.1038/nature02275.
- 1051 Hanan, B.B. and D.W. Graham (1996). Lead and Helium Isotope Evidence from Oceanic Basalts for a  
1052 Common Deep Source of Mantle Plumes. *Science* 272(5264): 991-995. DOI:  
1053 10.1126/science.272.5264.991
- 1054 Harpp, K.S. and W.M. White (2001). Tracing a mantle plume: Isotopic and trace element variations of  
1055 Galapagos seamounts. *Geochemistry Geophysics Geosystems* 2(2): Art.# 2000GC000137. 002001.  
1056 DOI: Artn 2000gc000137 Doi 10.1029/2000gc000137
- 1057 Harpp, K.S., P.S. Hall and M.G. Jackson (2014). Galápagos and Easter: A tale of two hotspots. *Galapagos*  
1058 *A Nat Lab Earth Sci* 204: 27-40.
- 1059 Harrison, L.N., D. Weis and M.O. Garcia (2017). The link between Hawaiian mantle plume composition,  
1060 magmatic flux, and deep mantle geodynamics. *Earth and Planetary Science Letters* 463: 298-309.  
1061 DOI: 10.1016/j.epsl.2017.01.027
- 1062 Hart, S.R., E.H. Hauri, L.A. Oschmann and J.A. Whitehead (1992). Mantle plumes and entrainment:  
1063 isotopic evidence. *Science* 256(5056): 517-520. DOI: 10.1126/science.256.5056.517.
- 1064 Hassan, R., N. Flament, M. Gurnis, D.J. Bower and D. Müller (2015). Provenance of plumes in global  
1065 convection models. *Geochemistry Geophysics Geosystems* 16(5): 1465-1489. DOI:  
1066 10.1002/2015gc005751
- 1067 Hassan, R., R.D. Müller, M. Gurnis, S.E. Williams and N. Flament (2016). A rapid burst in hotspot motion  
1068 through the interaction of tectonics and deep mantle flow. *Nature* 533, 239–241. DOI:  
1069 10.1038/nature17422
- 1070 Heron, P.J., J. Dannberg, R. Gassmöller, G.E. Shephard, J. van Hunen and R.N. Pysklywec (2019). Ancient  
1071 subducted oceans controlling the positioning of deep mantle plumes. DOI: 10.31223/osf.io/vdmys
- 1072 Hieronymus, C.F. and D. Bercovici (1999). Discrete alternating hotspot islands formed by interaction of  
1073 magma transport and lithospheric flexure. *Nature* 397(6720): 604-607. DOI: 10.1038/17584

- 1074 Hoernle, K., J. Rohde, F. Hauff, D. Garbe-Schonberg, S. Homrighausen, R. Werner and J.P. Morgan (2015).  
1075 How and when plume zonation appeared during the 132 Myr evolution of the Tristan Hotspot.  
1076 Nature Communications 6: 7799. DOI: 10.1038/ncomms8799
- 1077 Hoernle, K., R. Werner, J.P. Morgan, D. Garbe-Schonberg, J. Bryce and J. Mrazek (2000). Existence of  
1078 complex spatial zonation in the Galapagos plume for at least 14 m.y. Geology 28(5): 435-438. DOI:  
1079 Doi 10.1130/0091-7613(2000)28<435:Eocsi>2.0.Co;2
- 1080 Hofmann, A.W. and C.G. Farnetani (2013). Two views of Hawaiian plume structure. Geochemistry,  
1081 Geophysics, Geosystems 14(12): 5308-5322. DOI: 10.1002/2013gc004942
- 1082 Hofmann, A.W. and W.M. White (1982). Mantle Plumes from Ancient Oceanic-Crust. Earth and  
1083 Planetary Science Letters 57(2): 421-436. DOI: Doi 10.1016/0012-821x(82)90161-3.
- 1084 Holmes, A. (1928). Radioactivity and continental drift, Stephen Austin & Sons, Limited, printers.
- 1085 Holmes, A. (1931). XVIII. Radioactivity and earth movements. Transactions of the Geological Society of  
1086 Glasgow 18(3): 559-606.
- 1087 Horan, M.F., R.W. Carlson, R.J. Walker, M. Jackson, M. Garcon and M. Norman (2018). Tracking Hadean  
1088 processes in modern basalts with 142-Neodymium. Earth and Planetary Science Letters 484: 184-  
1089 191. DOI: 10.1016/j.epsl.2017.12.017.
- 1090 Huang, S.C., J. Farkas and S.B. Jacobsen (2011a). Stable calcium isotopic compositions of Hawaiian shield  
1091 lavas: Evidence for recycling of ancient marine carbonates into the mantle. Geochimica et  
1092 Cosmochimica Acta 75(17): 4987-4997. DOI: 10.1016/j.gca.2011.06.010.
- 1093 Huang, S.C., O. Tschauner, S.Y. Yang, M. Humayun, W.J. Liu, S.N.G. Corder, H.A. Bechtel and J. Tischler  
1094 (2020). HIMU geochemical signature originating from the transition zone. Earth and Planetary  
1095 Science Letters 542: 116323. DOI: ARTN 116323 10.1016/j.epsl.2020.116323
- 1096 Huang, S.C., P.S. Hall and M.G. Jackson (2011b). Geochemical zoning of volcanic chains associated with  
1097 Pacific hotspots. Nature Geoscience 4(12): 874-878. DOI: 10.1038/Ngeo1263
- 1098 Hull, P.M., A. Bornemann, D.E. Penman, M.J. Henehan, R.D. Norris, P.A. Wilson, P. Blum, L. Alegret, S.J.  
1099 Batenburg, P.R. Bown, T.J. Bralower, C. Cournede, A. Deutsch, B. Donner, O. Friedrich, S. Jehle, H.  
1100 Kim, D. Kroon, P.C. Lippert, D. Lorocho, I. Moebius, K. Moriya, D.J. Peppe, G.E. Ravizza, U. Röhl, J.D.  
1101 Schueth, J. Sepúlveda, P.F. Sexton, E.C. Sibert, K.K. Śliwińska, R.E. Summons, E. Thomas, T.  
1102 Westerhold, J.H. Whiteside, T. Yamaguchi and J.C. Zachos (2020). On impact and volcanism across  
1103 the Cretaceous-Paleogene boundary. Science 367(6475): 266. DOI: 10.1126/science.aay5055
- 1104 Ishii, M. and J. Tromp (2004). Constraining large-scale mantle heterogeneity using mantle and inner-core  
1105 sensitive normal modes. Physics of the Earth and Planetary Interiors 146(1-2): 113-124. DOI:  
1106 10.1016/j.pepi.2003.06.012
- 1107 Jackson, C.R.M., N.R. Bennett, Z.X. Du, E. Cottrell and Y.W. Fei (2018a). Early episodes of high-pressure  
1108 core formation preserved in plume mantle. Nature 553(7689): 491-+. DOI: 10.1038/nature25446
- 1109 Jackson, M.G., J.G. Konter and T.W. Becker (2017). Primordial helium entrained by the hottest mantle  
1110 plumes. Nature 542(7641): 340-343. DOI: 10.1038/nature21023
- 1111 Jackson, M.G., R.W. Carlson, M.D. Kurz, P.D. Kempton, D. Francis and J. Blusztajn (2010). Evidence for  
1112 the survival of the oldest terrestrial mantle reservoir. Nature 466(7308): 853-856. DOI:  
1113 10.1038/nature09287.

- 1114 Jackson, M.G., S.R. Hart, A.A. Koppers, H. Staudigel, J. Konter, J. Blusztajn, M. Kurz and J.A. Russell  
 1115 (2007). The return of subducted continental crust in Samoan lavas. *Nature* 448(7154): 684-687. DOI:  
 1116 10.1038/nature06048.
- 1117 Jackson, M.G., S.R. Hart, J.G. Konter, M.D. Kurz, J. Blusztajn and K.A. Farley (2014). Helium and lead  
 1118 isotopes reveal the geochemical geometry of the Samoan plume. *Nature* 514(7522): 355-358. DOI:  
 1119 10.1038/nature13794.
- 1120 Jackson, M.G., T.W. Becker and J.G. Konter (2018b). Geochemistry and Distribution of Recycled Domains  
 1121 in the Mantle Inferred From Nd and Pb Isotopes in Oceanic Hot Spots: Implications for Storage in the  
 1122 Large Low Shear Wave Velocity Provinces. *Geochemistry, Geophysics, Geosystems* DOI:  
 1123 10.1029/2018gc007552
- 1124 Jellinek, A.M. and M. Manga (2004). Links between long-lived hot spots, mantle plumes, D ", and plate  
 1125 tectonics. *Reviews of Geophysics* 42(3): Art. No. RG3002. DOI: 10.1029/2003rg000144
- 1126 Jellinek, A.M. and M.G. Jackson (2015). Connections between the bulk composition, geodynamics and  
 1127 habitability of Earth. *Nature Geoscience* 8(8): 587-593. DOI: 10.1038/Ngeo2488
- 1128 Jones, T.D., D.R. Davies and P.A. Sossi (2019). Tungsten isotopes in mantle plumes: Heads it's positive,  
 1129 tails it's negative. *Earth and Planetary Science Letters* 506: 255-267. DOI: 10.1016/j.epsl.2018.11.008
- 1130 Jones, T.D., D.R. Davies, I.H. Campbell, G. Iaffaldano, G. Yaxley, S.C. Kramer and C.R. Wilson (2017). The  
 1131 concurrent emergence and causes of double volcanic hotspot tracks on the Pacific plate. *Nature*  
 1132 545(7655): 472-476. DOI: 10.1038/nature22054
- 1133 Kennett, B.L.N., S. Widiyantoro and R.D. van der Hilst (1998). Joint seismic tomography for bulk sound  
 1134 and shear wave speed in the Earth's mantle. *Journal of Geophysical Research-Solid Earth* 103(B6):  
 1135 12469-12493. DOI: Doi 10.1029/98jb00150.
- 1136 Kerr, A.C. (2005). Oceanic LIPs: The Kiss of Death. *Elements* 1(5): 289-292. DOI:  
 1137 10.2113/gselements.1.5.289
- 1138 Kerr, A.C. (2014). Oceanic Plateaus. 631-667. DOI: 10.1016/b978-0-08-095975-7.00320-x
- 1139 Kim, D., V. Lekic, B. Menard, D. Baron and M. Taghizadeh-Popp (2020). Sequencing seismograms: A  
 1140 panoptic view of scattering in the core-mantle boundary region. *Science* 368(6496): 1223-1228. DOI:  
 1141 10.1126/science.aba8972
- 1142 King, S.D. and C. Adam (2014). Hotspot Swells Revisited. *Physics of the Earth and Planetary Interiors*(0)  
 1143 DOI: 10.1016/j.pepi.2014.07.006
- 1144 King, S.D. and G. Masters (1992). An Inversion for Radial Viscosity Structure Using Seismic Tomography.  
 1145 *Geophysical Research Letters* 19(15): 1551-1554. DOI: Doi 10.1029/92gl01700
- 1146 Koelemeijer, P., A. Deuss and J. Ritsema (2017). Density structure of Earth's lowermost mantle from  
 1147 Stoneley mode splitting observations. *Nat Commun* 8(1): 15241. DOI: 10.1038/ncomms15241
- 1148 Konrad, K., A.A.P. Koppers, B. Steinberger, V.A. Finlayson, J.G. Konter and M.G. Jackson (2018a). On the  
 1149 relative motions of long-lived Pacific mantle plumes. *Nature communications* 9(1): 854. DOI:  
 1150 10.1038/s41467-018-03277-x
- 1151 Konrad, K., Graham, D. W., Kent, A. J., & Koppers, A. A. (2018b). Spatial and temporal variability in  
 1152 Marquesas Islands volcanism revealed by <sup>3</sup>He/<sup>4</sup>He and the composition of olivine-hosted melt  
 1153 inclusions. *Chemical Geology*, 477, 161-176.

- 1154 Konter, J.G., A.J. Pietruszka, B.B. Hanan, V. Finlayson, P.R. Craddock, M.G. Jackson, N. Dauphas (2016).  
 1155 Unusual  $\delta^{56}\text{Fe}$  values in Samoan rejuvenated lavas generated in the mantle. *Earth Planet. Sci. Lett.*  
 1156 450, 221-232.
- 1157 Koppers, A.A.P. (2011). Mantle plumes persevere. *Nature Geoscience* 4(12): 816-817. DOI:  
 1158 10.1038/ngeo1334
- 1159 Koppers, A.A.P., H. Staudigel, M.S. Pringle and J.R. Wijbrans (2003). Short-lived and discontinuous  
 1160 intraplate volcanism in the South Pacific: Hot spots or extensional volcanism? *Geochemistry*  
 1161 *Geophysics Geosystems* 4(10) DOI: 10.1029/2003gc000533
- 1162 Koppers, A.A.P., J.A. Russell, J. Roberts, M.G. Jackson, J.G. Konter, D.J. Wright, H. Staudigel and S.R. Hart  
 1163 (2011a). Age Systematics of Two Young En Echelon Samoan Volcanic Trails. *Geochemistry*  
 1164 *Geophysics Geosystems*, doi:10.1029/2010GC003438.
- 1165 Koppers, A.A.P., J.P. Morgan, J.W. Morgan and H. Staudigel (2001). Testing the fixed hotspot hypothesis  
 1166 using  $^{40}\text{Ar}/^{39}\text{Ar}$  age progressions along seamount trails. *Earth and Planetary Science Letters* 185(3-  
 1167 4): 237-252. DOI: 10.1016/s0012-821x(00)00387-3
- 1168 Koppers, A.A.P., M.D. Gowen, L.E. Colwell, J.S. Gee, P.F. Lonsdale, J.J. Mahoney and R.A. Duncan  
 1169 (2011b). New  $^{40}\text{Ar}/^{39}\text{Ar}$  age progression for the Louisville hot spot trail and implications for inter-  
 1170 hot spot motion. *Geochemistry Geophysics Geosystems* 12 DOI: 10.1029/2011gc003804
- 1171 Koppers, A.A.P., T. Yamazaki, J. Geldmacher, J.S. Gee, N. Pressling, H. Hiroyuki and I.E.S. Party (2012).  
 1172 Limited Latitudinal Mantle Plume Motion for the Louisville Hotspot. *Nature Geoscience* DOI:  
 1173 10.1038/NGEO1638
- 1174 Kruijer, T.S. and T. Kleine (2018). No  $^{182}\text{W}$  excess in the Ontong Java Plateau source. *Chemical Geology*  
 1175 485: 24-31.
- 1176 Kumagai, I., A. Davaille, K. Kurita and E. Stutzmann (2008). Mantle plumes: Thin, fat, successful, or  
 1177 failing? Constraints to explain hot spot volcanism through time and space, *Geophysical Research*  
 1178 *Letters*, 35, L16301, DOI: 10.1029/2008GL035079.
- 1179 Kurz, M. D., Kenna, T. C., Lassiter, J. C., & DePaolo, D. J. (1996). Helium isotopic evolution of Mauna Kea  
 1180 Volcano: First results from the 1-km drill core. *Journal of Geophysical Research: Solid Earth*, 101(B5),  
 1181 11781-11791.
- 1182 Kurz, M.D., W.J. Jenkins and S.R. Hart (1982). Helium Isotopic Systematics of Oceanic Islands and Mantle  
 1183 Heterogeneity. *Nature* 297(5861): 43-47. DOI: DOI 10.1038/297043a0
- 1184 Larsen, T.B. and D.A. Yuen (1997). Fast plumeheads: Temperature-dependent versus non-Newtonian  
 1185 rheology. *Geophysical Research Letters* 24(16): 1995-1998. DOI: Doi 10.1029/97gl01886.
- 1186 Larson, R.L. (1991a). Geological Consequences of Superplumes. *Geology* 19(10): 963-966. DOI: Doi  
 1187 10.1130/0091-7613(1991)019<0963:Gcos>2.3.Co;2.
- 1188 Larson, R.L. (1991b). Latest pulse of Earth: Evidence for a mid-Cretaceous superplume. *Geology* 19(6):  
 1189 547-550. DOI: 10.1130/0091-7613(1991)019<0547:Lpoeef>2.3.Co;2
- 1190 Lau, H.C.P., J.X. Mitrovica, J.L. Davis, J. Tromp, H.Y. Yang and D. Al-Attar (2017). Tidal tomography  
 1191 constrains Earth's deep-mantle buoyancy. *Nature* 551(7680): 321-326. DOI: 10.1038/nature24452
- 1192 Lei, W., Y. Ruan, E. Bozdağ, D. Peter, M. Lefebvre, D. Komatitsch, J. Tromp, J. Hill, N. Podhorszki and D.  
 1193 Pugmire (2020). Global adjoint tomography—model GLAD-M25. *Geophysical Journal International*  
 1194 223(1): 1-21. DOI: 10.1093/gji/ggaa253.

- 1195 Lekic, V., S. Cottaar, A. Dziewonski and B. Romanowicz (2012). Cluster analysis of global lower mantle  
1196 tomography: A new class of structure and implications for chemical heterogeneity. *Earth and*  
1197 *Planetary Science Letters* 357-358: 68-77. DOI: 10.1016/j.epsl.2012.09.014
- 1198 Leng, W. and S.J. Zhong (2008). Controls on plume heat flux and plume excess temperature, *Journal of*  
1199 *Geophysical Research*, 113, B04408, DOI: 10.1029/2007JB005155
- 1200 Li, M., and S. Zhong (2017). The source location of mantle plumes from 3D spherical models of mantle  
1201 convection, *Earth and Planetary Science Letters*, 478, 47-57. DOI: 10.1016/j.epsl.2017.08.033
- 1202 Li, X.-D., and B. Romanowicz (1996) Global mantle shear velocity model developed using nonlinear  
1203 asymptotic coupling theory, *J. Geophys. Res.*, 101(B10), 22,245-22,272.
- 1204 Li, M.M. and S.J. Zhong (2017). The source location of mantle plumes from 3D spherical models of  
1205 mantle convection. *Earth and Planetary Science Letters* 478: 47-57. DOI: 10.1016/j.epsl.2017.08.033
- 1206 Li, M., A.K. McNamara, E.J. Garnero and S. Yu (2017). Compositionally-distinct ultra-low velocity zones  
1207 on Earth's core-mantle boundary. *Nat Commun* 8(1): 177. DOI: 10.1038/s41467-017-00219-x
- 1208 Li, Z. X., & Zhong, S. (2009). Supercontinent–superplume coupling, true polar wander and plume  
1209 mobility: plate dominance in whole-mantle tectonics. *Physics of the Earth and Planetary interiors*,  
1210 176(3-4), 143-156.
- 1211 Lin, S.-C. and P.E. van Keken (2006a). Dynamics of thermochemical plumes: 1. Plume formation and  
1212 entrainment of a dense layer, *Geochemistry, Geophysics, Geosystems*, 7, Q02006. DOI:  
1213 10.1029/2005GC001071
- 1214 Lin, S.-C., and P.E. van Keken (2006b), Dynamics of thermochemical plumes: 2. Complexity of plume  
1215 structures and its implications for mapping mantle plumes, *Geochemistry Geophysics Geosystems*,  
1216 7, Q03003, DOI: 10.1029/2005GC001072
- 1217 Lithgow-Bertelloni, C. and M.A. Richards (1998), The dynamics of Cenozoic and Mesozoic plate motions,  
1218 *Reviews of Geophysics* 36(1): 27-78, DOI: 10.1029/97RG02282
- 1219 Macpherson, C.G., D.R. Hilton, J.M. Sinton, R.J. Poreda and H. Craig (1998). High  $^3\text{He}/^4\text{He}$  ratios in the  
1220 Manus backarc basin: Implications for mantle mixing and the origin of plumes in the western Pacific  
1221 Ocean. *Geology* 26(11): 1007-1010.
- 1222 Mao, W.L., H.K. Mao, W. Sturhahn, J. Zhao, V.B. Prakapenka, Y. Meng, J. Shu, Y. Fei and R.J. Hemley  
1223 (2006). Iron-rich post-perovskite and the origin of ultralow-velocity zones. *Science* 312(5773): 564-  
1224 565. DOI: 10.1126/science.1123442
- 1225 Masters, G., G. Laske, H. Bolton and A. M. Dziewonski (2000) The Relative Behavior of Shear Velocity,  
1226 Bulk Sound Speed, and Compressional Velocity in the Mantle: Implications for Chemical and Thermal  
1227 Structure, in *Earth's Deep Interior: Mineral Physics and Tomography from the atomic to the global*  
1228 *scale*, AGU Volume 117, <https://doi.org/10.1029/GM117p0063>
- 1229 Matthews, K.J., K.T. Maloney, S. Zahirovic, S.E. Williams, M. Seton and D. Muller (2016). Global plate  
1230 boundary evolution and kinematics since the late Paleozoic. *Global and Planetary Change* 146: 226-  
1231 250. DOI: 10.1016/j.gloplacha.2016.10.002
- 1232 Mazza, S.E., E. Gazel, M. Bizimis, R. Moucha, P. Beguelin, E.A. Johnson, R.J. McAleer and A.V. Sobolev  
1233 (2019). Sampling the volatile-rich transition zone beneath Bermuda. *Nature* 569(7756): 398-403.  
1234 DOI: 10.1038/s41586-019-1183-6

- 1235 Mcdonough, W.F. and S.S. Sun (1995). The Composition of the Earth. *Chemical Geology* 120(3-4): 223-  
1236 253. DOI: Doi 10.1016/0009-2541(94)00140-4
- 1237 McNamara, A. and S. Zhong (2005), Thermochemical structures beneath Africa and the Pacific Ocean,  
1238 *Nature*, 437, 1136-1139, doi:10.1038/nature04066.
- 1239 McNamara, A.K. (2019). A review of large low shear velocity provinces and ultra low velocity zones.  
1240 *Tectonophysics* 760: 199-220. DOI: 10.1016/j.tecto.2018.04.015
- 1241 McNamara, A.K. and S.J. Zhong (2004). Thermochemical structures within a spherical mantle:  
1242 Superplumes or piles? *Journal of Geophysical Research-Solid Earth* 109(B7) DOI:  
1243 10.1029/2003jb002847
- 1244 McNutt, M.K. (1998). Superswells. *Reviews of Geophysics* 36(2): 211-244. DOI: 10.1029/98rg00255
- 1245 Meffre, S., T.J. Falloon, T.J. Crawford, K. Hoernle, F. Hauff, R.A. Duncan, S.H. Bloomer and D.J. Wright  
1246 (2012). Basalts erupted along the Tongan fore arc during subduction initiation: Evidence from  
1247 geochronology of dredged rocks from the Tonga fore arc and trench. *Geochemistry Geophysics*  
1248 *Geosystems* 13(12) DOI: Artn Q12003 10.1029/2012gc004335
- 1249 Minster, J.B. and T.H. Jordan (1978). Present-Day Plate Motions. *Journal of Geophysical Research*  
1250 83(Nb11): 5331-5354. DOI: DOI 10.1029/JB083iB11p05331
- 1251 Mitrovica, J.X. and A.M. Forte (2004). A new inference of mantle viscosity based upon joint inversion of  
1252 convection and glacial isostatic adjustment data. *Earth and Planetary Science Letters* 225(1-2): 177-  
1253 189. DOI: 10.1016/j.epsl.2004.06.005
- 1254 Montelli, R., G. Nolet, F.A. Dahlen and G. Masters (2006). A catalogue of deep mantle plumes: New  
1255 results from finite-frequency tomography. *Geochemistry Geophysics Geosystems* 7(11) DOI:  
1256 10.1029/2006gc001248
- 1257 Montelli, R., G. Nolet, F.A. Dahlen, G. Masters, E.R. Engdahl and S.H. Hung (2004). Finite-frequency  
1258 tomography reveals a variety of plumes in the mantle. *Science* 303(5656): 338-343. DOI:  
1259 10.1126/science.1092485
- 1260 Moore, W.B., G. Schubert and P. Tackley (1998). Three-dimensional simulations of plume-lithosphere  
1261 interaction at the Hawaiian swell. *Science* 279(5353): 1008-1011.
- 1262 Morgan, W.J. (1971). Convection Plumes in the Lower Mantle. *Nature* 230(5288): 42-43. DOI:  
1263 10.1038/230042a0
- 1264 Morgan, W.J. and J. Phipps Morgan, Plate velocities in the hotspot reference frame, G.R. Foulger, D.M.  
1265 Jurdy (Eds.), *Plates, Plumes, and Planetary Processes*, vol. 430, *Geol. Soc. of Am.*, Boulder, CO (2007),  
1266 pp. 65-78, DOI:10.1130/2007.2430(04).
- 1267 Mukhopadhyay, S. (2012). Early differentiation and volatile accretion recorded in deep-mantle neon and  
1268 xenon. *Nature* 486(7401): 101-104. DOI: 10.1038/nature11141
- 1269 Mukhopadhyay, S. and R. Parai (2019). Noble Gases: A Record of Earth's Evolution and Mantle  
1270 Dynamics. *Annual Review of Earth and Planetary Sciences*, Vol 47 47: 389-+. DOI: 10.1146/annurev-  
1271 earth-053018-060238
- 1272 Müller, R.D. (2010). Sedimentary basins feeling the heat from below. *Science* 329(5993): 769-770. DOI:  
1273 10.1126/science.1194560

- 1274 Müller, R.D., C. Gaina, W.R. Roest and D.L. Hansen (2001). A recipe for microcontinent formation.  
1275 *Geology* 29(3): 203-206. DOI: 10.1130/0091-7613(2001)029<0203:Armf>2.0.Co;2
- 1276 Müller, R.D., J.Y. Royer and L.A. Lawver (1993). Revised Plate Motions Relative to the Hotspots from  
1277 Combined Atlantic and Indian-Ocean Hotspot Tracks. *Geology* 21(3): 275-278. DOI: 10.1130/0091-  
1278 7613(1993)021<0275:Rpmrtt>2.3.Co;2
- 1279 Müller, R.D., M. Sdrolias, C. Gaina and W.R. Roest (2008). Age, spreading rates, and spreading  
1280 asymmetry of the world's ocean crust. *Geochemistry, Geophysics, Geosystems* 9(4): n/a-n/a. DOI:  
1281 10.1029/2007gc001743
- 1282 Mulyukova, E., B. Steinberger, M. Dabrowski and S.V. Sobolev (2015). Survival of LLSVPs for billions of  
1283 years in a vigorously convecting mantle: Replenishment and destruction of chemical anomaly.  
1284 *Journal of Geophysical Research: Solid Earth* 120: 3824-3847. DOI: 10.1002/2014jb011688
- 1285 Mundl, A., M. Touboul, M.G. Jackson, J.M. Day, M.D. Kurz, V. Lekic, R.T. Helz and R.J. Walker (2017).  
1286 Tungsten-182 heterogeneity in modern ocean island basalts. *Science* 356(6333): 66-69. DOI:  
1287 10.1126/science.aal4179
- 1288 Mundl-Petermeier, A., R.J. Walker, M.G. Jackson, J. Blichert-Toft, M.D. Kurz and S.A. Halldórsson (2019).  
1289 Temporal evolution of primordial tungsten-182 and 3He/4He signatures in the Iceland mantle  
1290 plume. *Chemical Geology* 525: 245-259. DOI: 10.1016/j.chemgeo.2019.07.026.
- 1291 Mundl-Petermeier, A., R.J. Walker, R.A. Fischer, V. Lekic, M.G. Jackson and M.D. Kurz (2020). Anomalous  
1292 182W in high 3He/4He ocean island basalts: Fingerprints of Earth's core? *Geochimica et*  
1293 *Cosmochimica Acta* 271: 194-211. DOI: 10.1016/j.gca.2019.12.020
- 1294 Nebel, O., P.A. Sossi, A. Benard, R.J. Arculus, G.M. Yaxley, J.D. Woodhead, D.R. Davies and S. Ruttor  
1295 (2019). Reconciling petrological and isotopic mixing mechanisms in the Pitcairn mantle plume using  
1296 stable Fe isotopes. *Earth and Planetary Science Letters* 521: 60-67. DOI: 10.1016/j.epsl.2019.05.037
- 1297 Nebel, O., R.J. Arculus, W. van Westrenen, J.D. Woodhead, F.E. Jenner, Y.J. Nebel-Jacobsen, M. Wille and  
1298 S.M. Eggins (2013). Coupled Hf-Nd-Pb isotope co-variations of HIMU oceanic island basalts from  
1299 Mangaia, Cook-Austral islands, suggest an Archean source component in the mantle transition zone.  
1300 *Geochimica et Cosmochimica Acta* 112: 87-101. DOI: 10.1016/j.gca.2013.03.005
- 1301 Nelson, P.L. and S.P., Grand (2018). Lower-mantle plume beneath the Yellowstone hotspot revealed by  
1302 core waves. *Nature Geoscience* 11: 280-284. DOI: 10.1038/s41561-018-0075-y
- 1303 Nemčok, M., S.T. Sinha, A.G. Doré, E.R. Lundin, J. Mascle and S. Rybár (2016). Mechanisms of  
1304 microcontinent release associated with wrenching-involved continental break-up; a review.  
1305 *Geological Society, London, Special Publications* 431(1): 323-359. DOI: 10.1144/sp431.14
- 1306 Ni, S., E. Tan, M. Gurnis and D. Helmberger (2002). Sharp sides to the African superplume. *Science*  
1307 296(5574): 1850-1852. DOI: 10.1126/science.1070698
- 1308 Nolet, G., F. Dahlen and R. Montelli (2005). Traveltimes and amplitudes of seismic waves: a re-  
1309 assessment. *GEOPHYSICAL MONOGRAPH-AMERICAN GEOPHYSICAL UNION* 157: 37
- 1310 Norton, I.O. (1995). Plate motions in the North Pacific: The 43 Ma nonevent. *Tectonics* 14(5), 1080-  
1311 1094, DOI: 10.1029/95TC01256
- 1312 O'Connor, J.M., B. Steinberger, M. Regelous, A.A.P. Koppers, J.R. Wijbrans, K.M. Haase, P. Stoffers, W.  
1313 Jokat and D. Garbe-Schönberg (2013). Constraints on past plate and mantle motion from new ages

- 1314 for the Hawaiian-Emperor Seamount Chain. *Geochemistry, Geophysics, Geosystems* 14(10): 4564-  
1315 4584. DOI: 10.1002/ggge.20267
- 1316 Olson, P. and D.A. Yuen (1982). Thermochemical Plumes and Mantle Phase-Transitions. *Journal of*  
1317 *Geophysical Research* 87(Nb5): 3993-4002. DOI: 10.1029/JB087iB05p03993
- 1318 Parnell-Turner, R., N. White, T. Henstock, B. Murton, J. Maclennan and S.M. Jones (2014). A continuous  
1319 55-million-year record of transient mantle plume activity beneath Iceland. *Nature Geoscience* 7(12):  
1320 914-919. DOI: 10.1038/Ngeo2281
- 1321 Payne, J. A., Jackson, M. G., & Hall, P. S. (2013). Parallel volcano trends and geochemical asymmetry of  
1322 the Society Islands hotspot track. *Geology*, 41(1), 19-22.
- 1323 Peate, D.W. (1997). The Parana-Etendeka Province. In: J. J. Mahoney; M. F. Coffin: Large Igneous  
1324 Provinces: continental, oceanic, and planetary flood volcanism. *Geophysical Monograph*, vol. 100,  
1325 American Geophysical Union, Washington, DC: 217-245.
- 1326 Peters, B.J., R.W. Carlson, J.M.D. Day and M.F. Horan (2018). Hadean silicate differentiation preserved  
1327 by anomalous Nd-142/Nd-144 ratios in the Reunion hotspot source. *Nature* 555(7694): 89-93. DOI:  
1328 10.1038/nature25754
- 1329 Petersen, K.D., S.B. Nielsen, O.R. Clausen, R. Stephenson and T. Gerya (2010). Small-Scale Mantle  
1330 Convection Produces Stratigraphic Sequences in Sedimentary Basins. *Science* 329(5993): 827-830.  
1331 DOI: 10.1126/science.1190115
- 1332 Pilet, S., M.B. Baker and E.M. Stolper (2008). Metasomatized lithosphere and the origin of alkaline lavas.  
1333 *Science* 320(5878): 916-919. DOI: 10.1126/science.1156563
- 1334 Poore, H., N. White and J. Maclennan (2011). Ocean circulation and mantle melting controlled by radial  
1335 flow of hot pulses in the Iceland plume. *Nature Geoscience* 4(8): 558-561. DOI: 10.1038/Ngeo1161
- 1336 Reagan, M.K., D.E. Heaton, M.D. Schmitz, J.A. Pearce, J.W. Shervais and A.A.P. Koppers (2019). Forearc  
1337 ages reveal extensive short-lived and rapid seafloor spreading following subduction initiation. *Earth*  
1338 *and Planetary Science Letters* 506: 520-529. DOI: 10.1016/j.epsl.2018.11.020.
- 1339 Reichow, M.K., M.S. Pringle, A.I. Al'Mukhamedov, M.B. Allen, V.L. Andreichev, M.M. Buslov, C.E. Davies,  
1340 G.S. Fedoseev, J.G. Fitton, S. Inger, A.Y. Medvedev, C. Mitchell, V.N. Puchkov, I.Y. Safonova, R.A.  
1341 Scott and A.D. Saunders (2009). The timing and extent of the eruption of the Siberian Traps large  
1342 igneous province: Implications for the end-Permian environmental crisis. *Earth and Planetary*  
1343 *Science Letters* 277(1-2): 9-20. DOI: 10.1016/j.epsl.2008.09.030
- 1344 Ren, Z.Y., S. Ingle, E. Takahashi, N. Hirano and T. Hirata (2005). The chemical structure of the Hawaiian  
1345 mantle plume. *Nature* 436(7052): 837-840. DOI: 10.1038/nature03907.
- 1346 Renne, P.R., A.L. Deino, F.J. Hilgen, K.F. Kuiper, D.F. Mark, W.S. Mitchell, L.E. Morgan, R. Mundil and J.  
1347 Smit (2013). Time Scales of Critical Events Around the Cretaceous-Paleogene Boundary. *Science*  
1348 339(6120): 684-687. DOI: 10.1126/science.1230492
- 1349 Ribe, N.M. and U.R. Christensen (1999). The dynamical origin of Hawaiian volcanism. *Earth and*  
1350 *Planetary Science Letters* 171(4): 517-531. DOI: Doi 10.1016/S0012-821x(99)00179-X
- 1351 Ricard, Y., M. Richards, C. Lithgowbertelloni and Y. Lestunff (1993). A Geodynamic Model of Mantle  
1352 Density Heterogeneity. *Journal of Geophysical Research-Solid Earth* 98(B12): 21895-21909. DOI: Doi  
1353 10.1029/93jb02216

- 1354 Richards, M. A., & Engebretson, D. C. (1992). Large-scale mantle convection and the history of  
1355 subduction. *Nature*, 355(6359), 437–440. <https://doi.org/10.1038/355437a0>
- 1356 Richards, M.A., B.H. Hager and N.H. Sleep (1988). Dynamically Supported Geoid Highs over Hotspots -  
1357 Observation and Theory. *Journal of Geophysical Research-Solid Earth and Planets* 93(B7): 7690-  
1358 7708. DOI: 10.1029/JB093iB07p07690
- 1359 Richards, M.A., R.A. Duncan and V.E. Courtillot (1989). Flood basalts and hot-spot tracks: plume heads  
1360 and tails. *Science* 246(4926): 103-107. DOI: 10.1126/science.246.4926.103
- 1361 Ritsema, J. and R.M. Allen (2003). The elusive mantle plume. *Earth and Planetary Science Letters* 207(1-  
1362 4): 1-12. DOI: 10.1016/s0012-821x(02)01093-2
- 1363 Ritsema, J., A. Deuss, H.J. van Heijst and J.H. Woodhouse (2011). S40RTS: a degree-40 shear-velocity  
1364 model for the mantle from new Rayleigh wave dispersion, teleseismic traveltime and normal-mode  
1365 splitting function measurements. *Geophysical Journal International* 184(3): 1223-1236. DOI:  
1366 10.1111/j.1365-246X.2010.04884.x
- 1367 Rizo, H., D. Andrault, N.R. Bennett, M. Humayun, A. Brandon, I. Vlastelic, B. Moine, A. Poirier, M.A.  
1368 Bouhifd and D.T. Murphy (2019). 182W evidence for core-mantle interaction in the source of mantle  
1369 plumes. *Geochemical Perspectives Letters* 11: 6-11. DOI: 10.7185/geochemlet.1917
- 1370 Rizo, H., R.J. Walker, R.W. Carlson, M.F. Horan, S. Mukhopadhyay, V. Manthos, D. Francis and M.G.  
1371 Jackson (2016). Preservation of Earth-forming events in the tungsten isotopic composition of  
1372 modern flood basalts. *Science* 352(6287): 809-812. DOI: 10.1126/science.aad8563.
- 1373 Romanowicz, B. (2001). Can we resolve 3D density heterogeneity in the lower mantle? *Geophysical*  
1374 *Research Letters* 28(6): 1107-1110. DOI: 10.1029/2000gl012278.
- 1375 Rost, S., E.J. Garnero, Q. Williams and M. Manga (2005). Seismological constraints on a possible plume  
1376 root at the core-mantle boundary. *Nature* 435(7042): 666-669. DOI: 10.1038/nature03620.
- 1377 Rovere, A., P.J. Hearty, J. Austermann, J.X. Mitrovica, J. Gale, R. Moucha, A.M. Forte and M.E. Raymo  
1378 (2015). Mid-Pliocene shorelines of the US Atlantic Coastal Plain — An improved elevation database  
1379 with comparison to Earth model predictions. *Earth-Science Reviews* 145: 117-131. DOI:  
1380 10.1016/j.earscirev.2015.02.007
- 1381 Rudolph, M.L., V. Lekic and C. Lithgow-Bertelloni (2015). Viscosity jump in Earth's mid-mantle. *Science*  
1382 350(6266): 1349-1352. DOI: 10.1126/science.aad1929
- 1383 Sager, W.W., J. Zhang, J. Korenaga, T. Sano, A.A.P. Koppers, M. Widdowson and J.J. Mahoney (2013). An  
1384 immense shield volcano within the Shatsky Rise oceanic plateau, northwest Pacific Ocean. *Nature*  
1385 *Geosci advance online publication*(11): 976-981. DOI: 10.1038/ngeo1934
- 1386 Sager, W.W., Y. Huang, M. Tominaga, J.A. Greene, M. Nakanishi and J. Zhang (2019). Oceanic plateau  
1387 formation by seafloor spreading implied by Tamu Massif magnetic anomalies. *Nature Geoscience*  
1388 DOI: 10.1038/s41561-019-0390-y
- 1389 Samuel, H. and C.G. Farnetani (2003). Thermochemical convection and helium concentrations in mantle  
1390 plumes. *Earth and Planetary Science Letters* 207(1-4): 39-56. DOI: 10.1016/S0012-821x(02)01125-1.
- 1391 Schoene, B., M.P. Eddy, K.M. Samperton, C.B. Keller, G. Keller, T. Adatte and S.F.R. Khadri (2019). U-Pb  
1392 constraints on pulsed eruption of the Deccan Traps across the end-Cretaceous mass extinction.  
1393 *Science* 363(6429): 862-866. DOI: 10.1126/science.aau2422.

- 1394 Schubert, G., D. L. Turcotte, and P. Olson (2001). *Mantle Convection in the Earth and Planets*. Cambridge  
1395 Univ. Press, New York.
- 1396 Schubert, G., G. Masters, P. Olson and P. Tackley (2004). Superplumes or plume clusters? *Physics of the*  
1397 *Earth and Planetary Interiors* 146: 147-162. DOI: 10.1016/j.pepi.2003.09.025.
- 1398 Schuberth, B.S.A., H.P. Bunge and J. Ritsema (2009). Tomographic filtering of high-resolution mantle  
1399 circulation models: Can seismic heterogeneity be explained by temperature alone? *Geochemistry,*  
1400 *Geophysics, Geosystems* 10(5): n/a-n/a. DOI: 10.1029/2009gc002401
- 1401 Self, S. (2006). The effects and consequences of very large explosive volcanic eruptions. *Philos Trans A*  
1402 *Math Phys Eng Sci* 364(1845): 2073-2097. DOI: 10.1098/rsta.2006.1814
- 1403 Seton, M., R.D. Müller, S. Zahirovic, C. Gaina, T. Torsvik, G. Shephard, A. Talsma, M. Gurnis, M. Turner, S.  
1404 Maus and M. Chandler (2012). Global continental and ocean basin reconstructions since 200Ma.  
1405 *Earth-Science Reviews* 113(3-4): 212-270. DOI: 10.1016/j.earscirev.2012.03.002
- 1406 Sharp, W.D. and D.A. Clague (2006). 50-Ma initiation of Hawaiian-Emperor bend records major change  
1407 in Pacific plate motion. *Science* 313(5791): 1281-1284. DOI: 10.1126/science.1128489.
- 1408 Simmons, N.A., A.M. Forte, L. Boschi and S.P. Grand (2010). GyPSuM: A joint tomographic model of  
1409 mantle density and seismic wave speeds. *Journal of Geophysical Research-Solid Earth* 115(B12) DOI:  
1410 Artn B12310 10.1029/2010jb007631
- 1411 Sinton, C.W. and R.A. Duncan (1997). Potential links between ocean plateau volcanism and global ocean  
1412 anoxia at the Cenomanian-Turonian boundary. *Economic Geology and the Bulletin of the Society of*  
1413 *Economic Geologists* 92(7-8): 836-842. DOI: DOI 10.2113/gsecongeo.92.7-8.836.
- 1414 Sleep, N.H. (1990). Hotspots and Mantle Plumes - Some Phenomenology. *Journal of Geophysical*  
1415 *Research-Solid Earth and Planets* 95(B5): 6715-6736. DOI: 10.1029/JB095iB05p06715
- 1416 Sleep, N.H. (2003). Simple features of mantle-wide convection and the interpretation of lower-mantle  
1417 tomograms. *Comptes Rendus Geoscience* 335(1): 9-22. DOI: 10.1016/S1631-0713(03)00008-7.
- 1418 Sleep, N.H. (2006). Mantle plumes from top to bottom. *Earth-Science Reviews* 77(4): 231-271. DOI:  
1419 10.1016/j.earscirev.2006.03.007
- 1420 Sobolev, S.V., A.V. Sobolev, D.V. Kuzmin, N.A. Krivolutsкая, A.G. Petrunin, N.T. Arndt, V.A. Radko and  
1421 Y.R. Vasiliev (2011). Linking mantle plumes, large igneous provinces and environmental  
1422 catastrophes. *Nature* 477(7364): 312-316. DOI: 10.1038/nature10385
- 1423 Sprain, C.J., P.R. Renne, L. Vanderkluysen, K. Pande, S. Self and T. Mittal (2019). The eruptive tempo of  
1424 Deccan volcanism in relation to the Cretaceous-Paleogene boundary. *Science* 363(6429): 866-870.  
1425 DOI: 10.1126/science.aav1446.
- 1426 Šrámek, O., W.F. McDonough, E.S. Kite, V. Lekić, S.T. Dye and S. Zhong (2013). Geophysical and  
1427 geochemical constraints on geoneutrino fluxes from Earth's mantle. *Earth and Planetary Science*  
1428 *Letters* 361: 356-366. DOI: 10.1016/j.epsl.2012.11.001
- 1429 Steinberger, B. (2000). Plumes in a convecting mantle: Models and observations for individual hotspots.  
1430 *Journal of Geophysical Research-Solid Earth* 105(B5): 11127-11152. DOI: 10.1029/1999jb900398
- 1431 Steinberger, B. and M. Antretter (2006). Conduit diameter and buoyant rising speed of mantle plumes:  
1432 Implications for the motion of hotspots and shape of plume conduits, *Geochemistry Geophysics*  
1433 *Geosystems*, 7(1), Q11018, DOI: 10.1029/2006GC001409

- 1434 Steinberger, B. and R.J. O'Connell (1997). Changes of the Earth's rotation axis owing to advection of  
1435 mantle density heterogeneities. *Nature* 387(6629): 169-173. DOI: DOI 10.1038/387169a0
- 1436 Steinberger, B. and R.J. O'Connell (1998). Advection of plumes in mantle flow: implications for hotspot  
1437 motion, mantle viscosity and plume distribution. *Geophysical Journal International* 132(2): 412-434.  
1438 DOI: 10.1046/j.1365-246x.1998.00447.x
- 1439 Steinberger, B. and T.H. Torsvik (2012). A geodynamic model of plumes from the margins of Large Low  
1440 Shear Velocity Provinces. *Geochemistry Geophysics Geosystems* 13(1) DOI: Artn Q01w09  
1441 10.1029/2011gc003808
- 1442 Steinberger, B., C.P. Conrad, A.O. Tutu and M.J. Hoggard (2019a). On the amplitude of dynamic  
1443 topography at spherical harmonic degree two. *Tectonophysics* 760: 221-228. DOI:  
1444 10.1016/j.tecto.2017.11.032.
- 1445 Steinberger, B., M.L. Seidel and T.H. Torsvik (2017). Limited true polar wander as evidence that Earth's  
1446 nonhydrostatic shape is persistently triaxial. *Geophysical Research Letters* 44(2): 827-834. DOI:  
1447 10.1002/2016gl071937
- 1448 Steinberger, B., P.L. Nelson, S.P. Grand and W. Wang (2019). Yellowstone Plume Conduit Tilt Caused by  
1449 Large-Scale Mantle Flow. *Geochemistry, Geophysics, Geosystems* 20(12): 5896-5912. DOI:  
1450 10.1029/2019gc008490
- 1451 Steinberger, B., R. Sutherland and R.J. O'Connell (2004). Prediction of Emperor-Hawaii seamount  
1452 locations from a revised model of plate motion and mantle flow, *Nature*, 430, 167-173, DOI:  
1453 10.1038/nature02660
- 1454 Steinberger, B., T.H. Torsvik and T.W. Becker (2012). Subduction to the lower mantle - a comparison  
1455 between geodynamic and tomographic models, *Solid Earth* 3: 415-432, DOI: 10.5194/se-3-415-2012
- 1456 Storey, B.C. (1995). The Role of Mantle Plumes in Continental Breakup - Case-Histories from  
1457 Gondwanaland. *Nature* 377(6547): 301-308. DOI: DOI 10.1038/377301a0.
- 1458 Su, W.J. and A.M. Dziewonski (1997). Simultaneous inversion for 3-D variations in shear and bulk velocity  
1459 in the mantle. *Physics of the Earth and Planetary Interiors* 100(1-4): 135-156. DOI: Doi  
1460 10.1016/S0031-9201(96)03236-0.
- 1461 Tackley, P.J. (1998). in *The Core-Mantle Boundary Region*, M. Gurnis, M. E. Wysession, E. Knittle, B. A.  
1462 Buffett, Eds. (American Geophysical Union, Washington, DC, 1998), pp. 231-253.
- 1463 Tackley, P.J. (2008). Modelling compressible mantle convection with large viscosity contrasts in a three-  
1464 dimensional spherical shell using the yin-yang grid. *Physics of the Earth and Planetary Interiors*  
1465 171(1-4): 7-18. DOI: 10.1016/j.pepi.2008.08.005.
- 1466 Tan, E., M. Gurnis and L. Han (2002). Slabs in the lower mantle and their modulation of plume  
1467 formation, *Geochemistry Geophysics Geosystems*, 3(11), 1067, DOI: 10.1029/2001GC000238
- 1468 Tan, E., W. Leng, S.J. Zhong and M. Gurnis (2011). On the location of plumes and lateral movement of  
1469 thermochemical structures with high bulk modulus in the 3-D compressible mantle. *Geochemistry*  
1470 *Geophysics Geosystems* 12(7) DOI: 10.1029/2011gc003665.
- 1471 Tarduno, J. and A. Koppers (2019). When Hotspots Move: The New View of Mantle Dynamics Made  
1472 Possible by Scientific Ocean Drilling. *Oceanography* 32(1): 150-152. DOI: 10.5670/oceanog.2019.137

- 1473 Tarduno, J.A. and R.D. Cottrell (1997). Paleomagnetic evidence for motion of the Hawaiian hotspot  
1474 during formation of the Emperor seamounts. *Earth and Planetary Science Letters* 153(3-4): 171-180.  
1475 DOI: Doi 10.1016/S0012-821x(97)00169-6.
- 1476 Tarduno, J.A., R.A. Duncan, D.W. Scholl, R.D. Cottrell, B. Steinberger, T. Thordarson, B.C. Kerr, C.R. Neal,  
1477 F.A. Frey, M. Torii and C. Carvallo (2003). The Emperor Seamounts: Southward motion of the  
1478 Hawaiian hotspot plume in earth's mantle. *Science* 301(5636): 1064-1069. DOI:  
1479 10.1126/science.1086442
- 1480 Tatsumoto, M. (1978). Isotopic composition of lead in oceanic basalt and its implication to mantle  
1481 evolution. *Earth and Planetary Science Letters* 38(1): 63-87. DOI: 10.1016/0012-821x(78)90126-7.
- 1482 Tejada, M.L.G., J. Geldmacher, F. Hauff, D. Heaton, A.A.P. Koppers, D. Garbe Schonberg, K. Hoernle, K.S.  
1483 Heydolph (2016). Geochemistry and age of Shatsky, Hess, and Ojin Rise seamounts: Implications for  
1484 a connection between the Shatsky and Hess Rises. *Geochimica et Cosmochimica Acta*, 185, 302-327,  
1485 DOI: 10.1016/j.gca.2016.04.006
- 1486 Tetley, M.G., S.E. Williams, M. Gurnis, N. Flament and R.D. Muller (2019). Constraining Absolute Plate  
1487 Motions Since the Triassic. *Journal of Geophysical Research-Solid Earth* 124(7): 7231-7258. DOI:  
1488 10.1029/2019jb017442.
- 1489 Thorne, M.S., E.J. Garnero and S.P. Grand (2004). Geographic correlation between hot spots and deep  
1490 mantle lateral shear-wave velocity gradients. *Physics of the Earth and Planetary Interiors* 146(1-2):  
1491 47-63. DOI: 10.1016/j.pepi.2003.09.026
- 1492 Thorne, M.S., E.J. Garnero, G. Jahnke, H. Igel and A.K. McNamara (2013). Mega ultra low velocity zone  
1493 and mantle flow. *Earth and Planetary Science Letters* 364: 59-67. DOI: 10.1016/j.epsl.2012.12.034
- 1494 To, A., B. Romanowicz, Y. Capdeville and N. Takeuchi (2005). 3D effects of sharp boundaries at the  
1495 borders of the African and Pacific Superplumes: Observation and modeling. *Earth and Planetary  
1496 Science Letters* 233(1-2): 137-153. DOI: 10.1016/j.epsl.2005.01.037
- 1497 Torsvik, T. H., van der Voo, R., Preeden, U., Mac Niocaill, C., Steinberger, B., Doubrovine, P. V., van  
1498 Hinsbergen, D.J.J., Domeier, M., Gaina, C., Tovher, E., Meert, J.G., McCausland, P.J. and Cocks, L.R.M.  
1499 (2012), Phanerozoic polar wander, paleogeography and dynamics, *Earth-Science Reviews*, 114, 325-  
1500 368, doi:10.1016/j.earscirev.2012.06.007
- 1501 Torsvik, T.H., M.A. Smethurst, K. Burke and B. Steinberger (2006). Large igneous provinces generated  
1502 from the margins of the large low-velocity provinces in the deep mantle. *Geophysical Journal  
1503 International* 167(3): 1447-1460. DOI: 10.1111/j.1365-246X.2006.03158.x
- 1504 Torsvik, T.H., P.V. Doubrovine, B. Steinberger, C. Gaina, W. Spakman, and M. Domeier (2017). Pacific  
1505 plate motion change caused the Hawaiian-Emperor Bend, *Nature Communications* 8: 15660, DOI:  
1506 10.1038/ncomms15660
- 1507 Torsvik, T.H., R. van der Voo, P.V. Doubrovine, K. Burke, B. Steinberger, L.D. Ashwal, R. Trønnes, S.J.  
1508 Webb and A.L. Bull (2014). Deep mantle structure as a reference frame for movements in and on the  
1509 Earth, *Proceedings of the National Academy of Sciences USA*, 111, 8735-8740,  
1510 doi:10.1073/pnas.1318135111
- 1511 Touboul, M., I.S. Puchtel and R.J. Walker (2012). 182W evidence for long-term preservation of early  
1512 mantle differentiation products. *Science* 335(6072): 1065-1069. DOI: 10.1126/science.1216351.

- 1513 Trampert, J., F. Deschamps, J. Resovsky and D. Yuen (2004). Probabilistic tomography maps chemical  
 1514 heterogeneities throughout the lower mantle. *Science* 306(5697): 853-856. DOI:  
 1515 10.1126/science.1101996
- 1516 van der Hilst, R.D., S. Widiyantoro and E.R. Engdahl (1997). Evidence for deep mantle circulation from  
 1517 global tomography. *Nature* 386(6625): 578-584. DOI: 10.1038/386578a0
- 1518 van der Meer, D.G., D.J.J. van Hinsbergen and W. Spakman (2018). Atlas of the underworld: Slab  
 1519 remnants in the mantle, their sinking history, and a new outlook on lower mantle viscosity.  
 1520 *Tectonophysics* 723: 309-448. DOI: 10.1016/j.tecto.2017.10.004
- 1521 Wang, C.Z., R.G. Gordon, T. Zhang and L. Zheng (2019). Observational Test of the Global Moving Hot  
 1522 Spot Reference Frame. *Geophysical Research Letters* 46(14): 8031-8038. DOI:  
 1523 10.1029/2019gl083663.
- 1524 Wang, S.M., H.Z. Yu, Q. Zhang and Y.H. Zhao (2018). Absolute plate motions relative to deep mantle  
 1525 plumes. *Earth and Planetary Science Letters* 490: 88-99. DOI: 10.1016/j.epsl.2018.03.021.
- 1526 Wang, Y. and L.X. Wen (2004). Mapping the geometry and geographic distribution of a very low velocity  
 1527 province at the base of the Earth's mantle. *Journal of Geophysical Research-Solid Earth* 109(B10)  
 1528 DOI: Artn B10305 10.1029/2003jb002674
- 1529 Wegener, A. (1915). *Die Entstehung der Kontinente und Ozeane*. Braunschweig, Sammlung Vieweg Heft.
- 1530 Weis, D., M.O. Garcia, J.M. Rhodes, M. Jellinek and J.S. Scoates (2011). Role of the deep mantle in  
 1531 generating the compositional asymmetry of the Hawaiian mantle plume. *Nature Geoscience* 4(12):  
 1532 831-838. DOI: 10.1038/Ngeo1328
- 1533 Weiss, Y., C. Class, S.L. Goldstein and T. Hanyu (2016). Key new pieces of the HIMU puzzle from olivines  
 1534 and diamond inclusions. *Nature* 537(7622): 666-670. DOI: 10.1038/nature19113
- 1535 Werner, R., K. Hoernle, U. Barckhausen and F. Hauff (2003). Geodynamic evolution of the Galápagos hot  
 1536 spot system (Central East Pacific) over the past 20 m.y.: Constraints from morphology,  
 1537 geochemistry, and magnetic anomalies. *Geochemistry, Geophysics, Geosystems* 4(12) DOI:  
 1538 10.1029/2003gc000576.
- 1539 Wessel, P. and C.P. Conrad (2019). Assessing Models for Pacific Absolute Plate and Plume Motions.  
 1540 *Geochemistry, Geophysics, Geosystems* 20(12): 6016-6032. DOI: 10.1029/2019gc008647
- 1541 Wessel, P. and L.W. Kroenke (2008). Pacific absolute plate motion since 145 Ma: An assessment of the  
 1542 fixed hot spot hypothesis. *Journal of Geophysical Research-Solid Earth* 113(B6): B06101. DOI: Artn  
 1543 B06101 doi:10.1029/2007jb005499
- 1544 White, R. and McKenzie, D., 1989. Magmatism at rift zones: the generation of volcanic continental  
 1545 margins and flood basalts. *Journal of Geophysical Research: Solid Earth*, 94(B6), pp.7685-7729.
- 1546 White, W.M. (2010). Oceanic Island Basalts and Mantle Plumes: The Geochemical Perspective. *Annual*  
 1547 *Review of Earth and Planetary Sciences* 38(1): 133-160. DOI: 10.1146/annurev-earth-040809-152450
- 1548 White, W.M. and A.W. Hofmann (1982). Sr and Nd Isotope Geochemistry of Oceanic Basalts and Mantle  
 1549 Evolution. *Nature* 296(5860): 821-825. DOI: DOI 10.1038/296821a0
- 1550 Whitehead, J.A. (1982). Instabilities of fluid conduits in a flowing earth—are plates lubricated by the  
 1551 asthenosphere? *Geophysical Journal of the Royal astronomical Society*, 132, 415-433, DOI:  
 1552 10.1111/j.1365-246X.1982.tb04975.x

- 1553 Whittaker, J.M., S.E. Williams, J.A. Halpin, T.J. Wild, J.D. Stilwell, F. Jourdan and N.R. Daczko (2016).  
1554 Eastern Indian Ocean microcontinent formation driven by plate motion changes. *Earth and*  
1555 *Planetary Science Letters* 454: 203-212. DOI: 10.1016/j.epsl.2016.09.019
- 1556 Williams, C.D., S. Mukhopadhyay, M.L. Rudolph and B. Romanowicz (2019). Primitive Helium Is Sourced  
1557 From Seismically Slow Regions in the Lowermost Mantle. *Geochemistry Geophysics Geosystems*  
1558 20(8): 4130-4145. DOI: 10.1029/2019gc008437.
- 1559 Williams, Q. and E.J. Garnero (1996). Seismic evidence for partial melt at the base of Earth's mantle.  
1560 *Science* 273(5281): 1528-1530. DOI: DOI 10.1126/science.273.5281.1528
- 1561 Wilson, J.T. (1963). A possible origin of the Hawaiian Islands. *Canadian Journal of Physics* 41: 863-870.
- 1562 Wolfe, C.J., I.T. Bjarnason, J.C. VanDecar and S.C. Solomon (1997). Seismic structure of the Iceland  
1563 mantle plume. *Nature* 385(6613): 245-247. DOI: 10.1038/385245a0
- 1564 Wolfe, C.J., S.C. Solomon, G. Laske, J.A. Collins, R.S. Detrick, J.A. Orcutt, D. Bercovici and E.H. Hauri  
1565 (2009). Mantle Shear-Wave Velocity Structure Beneath the Hawaiian Hot Spot. *Science* 326(5958):  
1566 1388-1390. DOI: 10.1126/science.1180165
- 1567 Woodworth, D. and R.G. Gordon (2018). Paleolatitude of the Hawaiian Hot Spot Since 48 Ma: Evidence  
1568 for a Mid-Cenozoic True Polar Stillstand Followed by Late Cenozoic True Polar Wander Coincident  
1569 With Northern Hemisphere Glaciation. *Geophysical Research Letters* 45(21): 11632-11640. DOI:  
1570 10.1029/2018gl080787.
- 1571 Workman, R.K., J.M. Eiler, S.R. Hart and M.G. Jackson (2008). Oxygen isotopes in Samoan lavas:  
1572 Confirmation of continent recycling. *Geology* 36(7): 551-554. DOI: 10.1130/G24558a.1.
- 1573 Yang, J. and M. Faccenda (2020). Intraplate volcanism originating from upwelling hydrous mantle  
1574 transition zone. *Nature* 579(7797): 88-91. DOI: 10.1038/s41586-020-2045-y
- 1575 Yuan, K.Q. and B. Romanowicz (2017). Seismic evidence for partial melting at the root of major hot spot  
1576 plumes. *Science* 357(6349): 393-396. DOI: 10.1126/science.aan0760
- 1577 Zhang, N., S.J. Zhong, W. Leng and Z.X. Li (2010). A model for the evolution of the Earth's mantle  
1578 structure since the Early Paleozoic. *Journal of Geophysical Research-Solid Earth* 115(B6) DOI: Artn  
1579 B06401 10.1029/2009jb006896.
- 1580 Zhong, S.J. (2006). Constraints on thermochemical convection of the mantle from plume heat flux,  
1581 plume excess temperature and upper mantle temperature, *Journal of Geophysical Research*, 111,  
1582 B04409. DOI: 10.1029/2005JB003972
- 1583 Zhong, S.J., M.T. Zuber, L. Moresi and M. Gurnis (2000). Role of temperature-dependent viscosity and  
1584 surface plates in spherical shell models of mantle convection. *Journal of Geophysical Research-Solid*  
1585 *Earth* 105(B5): 11063-11082. DOI: Doi 10.1029/2000jb900003.
- 1586 Ziegler, P.A. and S. Cloetingh (2004). Dynamic processes controlling evolution of rifted basins. *Earth-*  
1587 *Science Reviews* 64(1-2): 1-50. DOI: 10.1016/S0012-8252(03)00041-2.
- 1588 Zindler, A. and S. Hart (1986). Chemical geodynamics. *Annual Review Earth and Planetary Science* 14:  
1589 493-571. DOI: 10.1146/annurev.ea.14.050186.002425